DOI: 10.1534/genetics.106.061812

A ONECUT Homeodomain Protein Communicates X Chromosome Dose to Specify *Caenorhabditis elegans* Sexual Fate by Repressing a Sex Switch Gene

John M. Gladden and Barbara J. Meyer[1]

Howard Hughes Medical Institute, Department of Molecular and Cell Biology, University of California, Berkeley, California 94720-3204

Manuscript received June 22, 2007
Accepted for publication August 8, 2007

ABSTRACT

Sex is determined in *Caenorhabditis elegans* through a dose-dependent signal that communicates the number of X chromosomes relative to the ploidy, the number of sets of autosomes. The sex switch gene *xol-1* is the direct molecular target of this X:A signal and integrates both X and autosomal components to determine sexual fate. X chromosome number is relayed by X signal elements (XSEs) that act cumulatively to repress *xol-1* in XX animals, thereby inducing hermaphrodite fate. Ploidy is relayed by autosomal signal elements (ASEs), which counteract the single dose of XSEs in XO animals to activate *xol-1* and induce the male fate. Our goal was to identify and characterize new XSEs and further analyze known XSEs to understand the principles by which a small difference in the concentration of an intracellular signal is amplified to induce dramatically different developmental fates. We identified a new XSE, the ONECUT homeodomain protein CEH-39, and showed that it acts as a dose-dependent repressor of *xol-1* transcript levels. Unexpectedly, most other XSEs also repress *xol-1* predominantly, but not exclusively, at the transcript level. The twofold difference in X dose between XO and XX animals is translated into the male *vs.* hermaphrodite fate by the synergistic action of multiple, independent XSEs that render *xol-1* active or inactive, primarily through transcriptional regulation.

DURING development, different concentrations of select dose-dependent signals can induce alternative cell fates. Among the classes of dose-dependent signals are those that invoke cell–cell communication to determine developmental fate and those that originate and function within the cell to specify fate. In the first class, signaling molecules secreted from one group of cells influence intracellular signaling cascades in neighboring cells. For example, the *Wnt*-signaling pathway patterns the dorsal–ventral axis of the Drosophila wing in a concentration-dependent manner. In the second class, gradients of the Drosophila morphogens Bicoid and Nanos exemplify intracellular signals. They control expression of early patterning genes in a concentration-dependent manner to establish anterior–posterior polarity in the embryo (Parisi and Lin 2000; Lynch and Desplan 2003). Defining the molecular nature of dose-dependent signals and their sensors is therefore paramount to understanding cell fate specification in multi-cellular organisms.

Sex-determination strategies reliant on chromosome complement provide further opportunities to dissect mechanisms by which small, quantitative differences in an intracellular signal are translated into alternative developmental fates. For example, in *Drosophila melanogaster* and *Caenorhabditis elegans*, chromosome counting mechanisms distinguish one X chromosome from two to specify male (XY or XO) *vs.* female/hermaphrodite (XX) fate. Both organisms tally the number of X chromosomes relative to the sets of autosomes (Madl and Herman 1979), the X:A ratio, using X-linked genes called X signal elements (XSEs) to communicate the X chromosome number and autosomal signal elements (ASEs) to communicate the ploidy. In *D. melanogaster*, the double dose of four XSEs (*sisA*, *sisB*, *sisC*, and *runt*) in diploid XX embryos (X:A = 1.0) activates transcription of the sex switch gene *Sex-lethal* to induce female development. The single dose of XSEs in diploid XY animals (X:A = 0.5) is insufficient to activate *Sex-lethal*, thereby permitting the male fate (Cline and Meyer 1996).

In *C. elegans*, the sex switch gene *xol-1* is the direct molecular target of the X:A signal and integrates both X and autosomal components to determine sexual fate. Two copies of XSEs, including the nuclear receptor SEX-1 and the RNA-binding protein FOX-1, induce the hermaphrodite fate in diploid XX embryos by repressing *xol-1* through transcriptional and post-transcriptional mechanisms, respectively (Figure 1; Akerib and Meyer 1994; Hodgkin *et al.* 1994; Nicoll *et al.* 1997; Carmi *et al.* 1998). The single copy of XSEs in diploid XO embryos cannot overcome *xol-1* activation by the double dose of ASEs, thereby permitting the male fate.

[1]*Corresponding author:* Department of Molecular and Cell Biology, Howard Hughes Medical Institute, 16 Barker Hall, MC 3204, University of California, Berkeley, CA 94720-3204. E-mail: bjmeyer@berkeley.edu

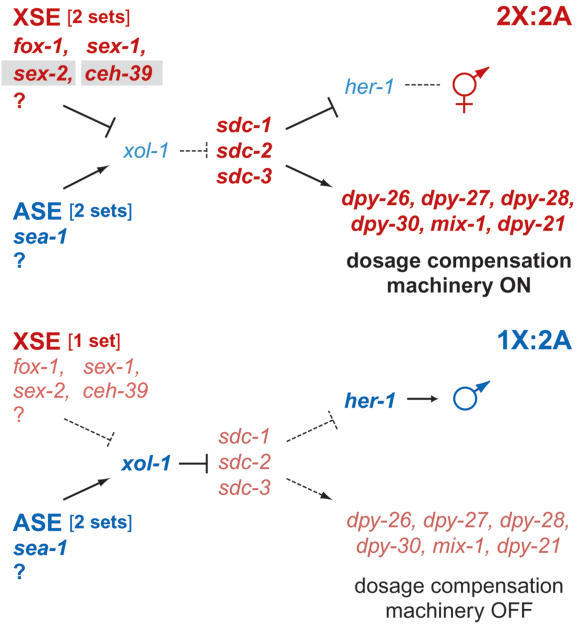

Figure 1.—The genetic pathway for sex determination and dosage compensation in *C. elegans*. This pathway includes our discovery of *ceh-39* as an XSE and partial analysis of the XSE *sex-2*; both XSEs are highlighted by gray boxes. In XX animals (top), the two copies of the X-linked XSE genes repress *xol-1*, permitting activation of the *sdc* genes. The SDC proteins trigger assembly of the dosage compensation complex (SDC-1, SDC-2, SDC-3, DPY-21, DPY-26, DPY-27, DPY-28, DPY-30, MIX-1) on X, where it reduces gene expression by half. SDC proteins also promote the hermaphrodite fate by repressing *her-1*, a male sex determination gene. In XO animals (bottom), the single copy of XSEs allows the ASEs to activate *xol-1*. When *xol-1* is active, the *sdc* genes are repressed, promoting the male fate by permitting *her-1* expression and preventing assembly of the dosage compensation machinery on X. The genes in boldface type are active in a specific sex. Genes in red type are required for hermaphrodite development; genes in blue type are required for male development.

One of the ASEs, the T-box transcription factor SEA-1 (*s*ignal *e*lement on *a*utosome), helps activate *xol-1* by increasing its transcript levels (Powell *et al.* 2005). The X:A signal includes two other partially characterized components, the XSE *sex-2* (J. Powell, C. Y. Loh and B. Meyer, unpublished results) and the ASE *sea-2* (P. Nix and B. Meyer, unpublished results).

The worm sex-determination mechanism discriminates with great accuracy between small differences in the X:A signal. An X:A of 0.67 dictates male fate and an X:A of 0.75 dictates hermaphrodite fate, implying that the effectiveness of the signal might derive from the combined action of multiple X and autosomal elements. Indeed, previous genetic analysis provided evidence that additional X signal elements exist, but did not identify the specific genes (Akerib and Meyer 1994; Carmi and Meyer 1999). Our goal in this study was to identify and characterize new XSEs and to further analyze known XSEs to understand the principles by which intracellular signals can induce different developmental fates in a concentration-dependent manner.

Analysis of the X:A signal is complicated by the fact that the signal controls viability as well as sexual fate. In addition to controlling sex determination, *xol-1* controls X chromosome dosage compensation, the vital process that equalizes X-linked gene products between XX and XO animals by halving gene expression from both hermaphrodite X chromosomes (reviewed in Meyer 2005). In XX animals, a decrease in XSE dose or an increase in ASE dose can activate *xol-1*, prevent dosage compensation, and cause XX lethality. In XO animals, an increase in XSE dose or a decrease in ASE dose can repress *xol-1*, activate the dosage compensation machinery, and cause XO lethality.

In XO animals, *xol-1* sets the male fate by repressing the hermaphrodite-specific *sdc* genes, which coordinately control downstream genes specialized for regulating either sex determination or dosage compensation (Figure 1). In XX animals, where *xol-1* is repressed, SDC-2 induces hermaphrodite development by repressing the male-specific sex-determination gene *her-1* and by triggering assembly of the dosage compensation complex (DCC) on both X chromosomes to repress transcript levels. The DCC includes two other SDC proteins and at least seven other dosage compensation proteins, five of which resemble the components of condensin, a conserved protein complex required for mitotic and meiotic chromosome compaction, resolution, and segregation (Villeneuve and Meyer 1987, 1990; Nusbaum and Meyer 1989; Nonet and Meyer 1991; Delong *et al.* 1993; Chuang *et al.* 1994; Hsu and Meyer 1994; Lieb *et al.* 1996, 1998; Davis and Meyer 1997; Kimura and Hirano 1997; Dawes *et al.* 1999; Hirano 1999; Chu *et al.* 2002; Yonker and Meyer 2003; M. Albrecht, C. Hassig, C. Tsai and B. Meyer, unpublished results). The DCC binds to recruitment sites on X and then appears to spread in *cis* to X regions lacking recruitment sites (Csankovszki *et al.* 2004; McDonel *et al.* 2006).

Previous studies indicated that the sensitivity and fidelity of X chromosome counting stems from two characteristics: (1) multiple XSEs collaborate to communicate X dose and (2) XSEs use multiple mechanisms to regulate one gene, *xol-1*. The XSEs act in a cumulative manner to repress *xol-1*: changing the dose of individual XSEs has little effect on sex determination and dosage compensation, but changing the dose of multiple XSEs has synergistic effects, causing sexual transformation and death (Akerib and Meyer 1994; Carmi and Meyer 1999).

Many principles underlying X chromosome counting have emerged, but a detailed mechanistic picture has not. In our study, we identified the new XSE CEH-39, a ONECUT (OC) homeodomain protein, and further analyzed known XSEs to learn how the X chromosome counting process functions with high precision. Although previous studies showed that both transcriptional and

post-transcriptional modes of *xol-1* regulation are important, they did not address the relative contribution of each mechanism to *xol-1* repression. Our study showed that CEH-39 and most other XSEs communicate X chromosome dose by repressing *xol-1* predominately at the transcript level.

MATERIALS AND METHODS

Strains and general methods: All *C. elegans* strains were derived from the Bristol variant N2 and were maintained as described in Brenner (1974). Abbreviations are as follows: *ceh* (***C.*** ***e****legans* **h**omeobox), *dpy* (*d*um*py*), *egl* (*e*gg-*l*aying defective), *fasn* (*f*atty *a*cid *sy**n*thase), *fox* (*f*eminizing gene *o*n *X*), *him* (*h*igh *i*ncidence of *m*ales), *lon* (*lon*g), *nhr* (*n*uclear *h*ormone *r*eceptor), *sdc* (*s*ex determination and *d*osage *c*ompensation), *sea* (*s*ignal *e*lement on *a*utosome), *sex* (*s*ignal *e*lement on *X*), *tra* (sexual *tra*nsformation), *unc* (*unc*oordinated), and *xol* (*XO* *l*ethal). The following chromosomal aberrations and mutations were used for this study:

LG II: *sea-1(y356)* (Powell *et al.* 2005).
LG III: *dpy-27(y57)* (Plenefisch *et al.* 1989), *yIs33*[*Pxol-1::lacZ*] (Nicoll *et al.* 1997).
LG IV: *him-8(e1489), mIs11, yIs2*[*xol-1::lacZ*] (Rhind *et al.* 1995), *yIs58*[*ceh-39(+), myo-2::gfp*]. *him-8(e1489)* increases X chromosome nondisjunction, resulting in 37% XO, 57% XX, and 6% Dpy XXX animals (Hodgkin *et al.* 1979). *mIs11* is a multi-construct array carrying *myo-2::gfp, pes-10::gfp,* and *gut::gfp* integrated onto LG IV near *dpy-20. yIs58* is an integrated array carrying the wild-type *ceh-39* gene and the co-injection marker *myo-2::gfp.*
LG X: *dpy-3(e27), unc-2(e55), ceh-39(y414), ceh-39(gk296)* (Vancouver group of the *C. elegans* Gene Knockout Consortium), *fox-1(y303)* (Nicoll *et al.* 1997), *sex-2(y324)* (J. Powell and B. Meyer, unpublished results), *lon-2(e678), xol-1(y9)* (Miller *et al.* 1988), *dpy-6(e14), sex-1(y263)* (Carmi *et al.* 1998).
Duplication: *yDp14(X;I)* (Akerib and Meyer 1994).
Rearrangement: *szT1(I;X)* (McKim *et al.* 1988).
Extrachromosomal array: *yEx483*[*Pdpy-30::sdc-2(+), myo-2::gfp(+), rol-6(d)*] (Powell *et al.* 2005).

Mutations not referenced are described in this study or in Riddle *et al.* (1997).

Isolation of *ceh-39(y414)*: A *C. elegans* deletion library was constructed in the Meyer Lab and screened for a *ceh-39* deletion following Michael Koelle's *C. elegans* Gene Knockout Protocol (02/09/03 update) retrieved from his Yale University website (http://info.med.yale.edu/mbb/koelle/). *ceh-39* primers used were as follows:

Forward outer primer: GAAATTTACGCTGGCCGTCTGC;
Reverse outer primer: GCCTCTGGATTTCTTTGCTGG;
Forward inner primer: TCTCCGTGCGCTATTTAGGTGC;
Reverse inner primer: TATGGAAGCAGAGCATCGTTGG;
Poison primer 1: CGGTATGTGTTGGAGAAGTCCA;
Poison primer 2: AGAGGTCGTCGACTTCCCAGAG.

RNA interference: Generally, RNA interference (RNAi) was conducted as described in Kamath *et al.* (2001), except carbenicillin (25 μg/ml) was used without tetracycline in the overnight cultures. The double-stranded (dsRNA) synthesis was induced in *Escherichia coli* on plates (1 mm IPTG, 25 μg/ml carbenicillin) incubated overnight at 25°. Bacterial plasmids were constructed or obtained from an Ahringer RNAi feeding library (Kamath and Ahringer 2003). Embryos were placed onto plates with the dsRNA-producing *E. coli* until they became gravid hermaphrodites (24–36 hr at 20°). Next, two hermaphrodites were picked onto each of six plates with dsRNA-producing *E. coli* and allowed to lay embryos for 24 hr. The laid embryos were counted, and the resulting animals were scored over a 5-day period to maximize viability estimates for slow-growing worms.

For the matings, males (five per hermaphrodite) were placed onto the original plates containing embryos and dsRNA-producing *E. coli* once the embryos reached L4. Twenty-four hours later, two gravid, mated hermaphrodites and 10 males were transferred to each of six plates and allowed to mate and lay embryos for 24 hr. The laid embryos were counted. As the animals reached L4, they were picked off and scored. Any animal that failed to reach L4 after 5 days was considered inviable. For progeny counts pertaining to either matings or self-fertilization, the embryos and adults scored for each plate were summed to generate the *n* values reported in each table, except for strains for which viability was reported with a standard deviation or error of the mean. In those cases, the viability presented is an average of the numbers from the six plates.

For simultaneous RNAi against the three genes *ceh-21, ceh-41,* and *ceh-39,* dsRNA corresponding to these genes was injected into the gonads of L4 hermaphrodites. dsRNA was synthesized *in vitro* with the T7 RiboMAX Large Scale Production System from Promega (Madison, WI) using the Ahringer RNAi feeding construct plasmid DNA as template. dsRNA corresponding to each of these genes was mixed in a 1:1:1 ratio prior to injection. Embryos laid 12–36 hr post-injection were counted, and the resulting adults scored.

Statistical analysis: Statistical comparisons were made using the χ^2 test, except for experiments involving quantitative RT–PCR (qRT–PCR) measurement of transcript levels, which utilized the Student's *t*-test.

Construction of *yIs58*: *yIs58* is a UV integrant of the extrachromosomal array *yEx689. yEx689* was generated by co-injecting pPD118.33 *myo-2::gfp(+)* (50 ng/μl) and pJG75 (50 ng/μl), a plasmid containing a 5.5-kbp genomic PCR fragment spanning the *ceh-39* locus amplified with primers (forward, TTTCGGCAA GAGTGCTCTGAAC; reverse, TTGGAATAGAGAAGAGAGC GAC). UV integration involved the following protocol adapted from Andrew Frank. *yEx689* worms were washed four times in M9. The worms were then spun down and resuspended in a small volume for plating on an unseeded 9-cm plate. Worms were irradiated without the plate lid using a Stratalinker UV crosslinker (Stratagene, La Jolla, CA) with a UV dose of 15–35 mJ/cm^2. OP50 bacteria were then added to the plate, and worms were allowed to recover at room temperature for 5 hr. Transgenic L4 larvae or young adult P0's were plated at a density of two or three per plate on 10–30 plates and allowed to lay F_1 progeny, which were then picked individually onto 150 fresh plates. Finally, 2–3 F_2 progeny from one F_1 plate were picked individually onto 300 fresh plates. Of 300 F_2's, 1 segregated 100% GFP-positive animals. The integrated transgene was designated *yIs58.*

β-Galactosidase staining: β-Galactosidase activity was used to assess the degree of *xol-1* derepression in the reporters *yIs2* and *yIs33* using X-gal (5-bromo-4-chloro-3-indolyl-β-D-galactopyranoside) as the chromogenic substrate for β-galactosidase. *yIs2* XX, *yIs2; ceh-39(y414)* XX, *him-8(e1489) yIs2* XX, *yIs33* XX, *yIs33; him-8(e1489)* XX, and *yIs33; ceh-39(y414)* XX worms were prepared using the following protocol: Worms were placed into a multi-welled glass dish and dried by placing under vacuum for 30 min. Desiccated worms were incubated with −20° acetone for 5 min and allowed to air dry. Worms were then stained by adding staining solution (recipe below) and incubated at 35° for 5–7 hr in a sealed humidified container. The *yIs2* and *yIs33 him-8* strains were used to control for the time of the β-galactosidase reaction. When the *him-8* animals

had several darkly stained XO embryos, all reactions were stopped by exchanging the staining solution with H_2O. Worms were transferred with a Pasteur pipette to glass slides for microscopy. A worm was considered to have high β-galactosidase activity if it had at least one darkly staining embryo; worms with fewer than three embryos were not scored. The staining solution was prepared from the following: 500 μl 2× phosphate buffer (360 mM Na_2HPO_4, 40 mM NaH_2PO_4), 400 μl H_2O, 100 μl of 100 mM Redox buffer (50 mM potassium ferricyanide, 50 mM potassium ferrocyanide), 10 μl of 1 M $MgCl_2$, 4 μl 1% SDS, 2 μl of 1 mg/ml 4′,6-diamidino-2-phenylindole (DAPI), 12 μl of 2% X-gal (5-bromo-4-chloro-3-indolyl-β-D-galactopyranoside) in *N,N*-dimethylformamide, and 5 μl of 50 mg/ml kanamycin sulfate).

Quantification of transcript levels: qRT–PCR was used to measure transcript levels from RNA isolated from three independent growths of the strains listed in Table 7. The protocol of Van Gilst *et al.* (2005) was used, except that worms were grown on egg plates (http://www.wormbook.org) prior to isolating the mixed-stage embryos, and the total RNA was treated with DNase prior to cDNA synthesis using 3 μl of RQ1 RNase-free DNase (Promega)/100 μg of RNA in a 50-μl reaction, as per manufacturer's instructions. For each strain tested, 5 μg of total RNA were used to generate cDNA. Primer sequences are available upon request.

Transcript levels of genes indicated in Table 7 were normalized to the transcript level of the *f*atty *a*cid *syn*thase gene *fasn-1* [open reading frame (ORF) F32H2.5], which is expressed constitutively throughout embryogenesis, by adjusting the cycle threshold (Ct) value of *fasn-1*, measured in each strain to equal the Ct value of *fasn-1* measured in wild-type animals. The Ct values of all other transcripts measured in the same strain were then adjusted by the same amount. This adjustment equalizes the small variations in concentration of the starting material added to each PCR reaction from different RNA preparations.

The transcript level of each mutant strain was then expressed as fold change relative to wild-type animals (ΔCt). The normalized Ct value for each transcript measured in each strain was subtracted from the normalized Ct value of the same transcript measured in wild-type animals. The difference between these values corresponds to the change in transcript levels relative to those in wild-type animals. Ct values are expressed as PCR cycle numbers. Each PCR cycle increases the concentration of the template by twofold. Therefore, to convert the difference in Ct values to a relative change in concentration, the expression $2^{\Delta Ct}$ was used.

CEH-39 antibody: Two separate rabbit anti-CEH-39 antibodies (CA1184 and CA1183) were raised (Covance) against a 28-amino-acid peptide including the CEH-39 N terminus plus a GC linker (DFSNTYRNYGEVVDFPEDFESDYVPTVKGC). Both antibodies were affinity purified using the same peptide, which was synthesized by David King (University of California, Berkeley). Both antibodies yielded similar staining patterns. For neither antibody was staining detectable in mutants carrying the *ceh-39(y414)* deletion, which eliminates the DNA encoding the peptide. CA1184 was used for Westerns and embryo staining (Figure 4, A–D). CA1183 was used for gonad staining (Figure 4, E and F).

Immunofluorescence microscopy: Embryos were fixed as described in Davis and Meyer (1997) and stained as described in Chuang *et al.* (1994), except that both the primary and the secondary antibody staining were done overnight. The following antibodies were used: rabbit anti-CEH-39, rabbit anti-DPY-27 (Chuang *et al.* 1994), rat anti-SDC-3 (McDonel *et al.* 2006), FITC-conjugated goat anti-rabbit (Jackson ImmunoResearch Labs), and Cy5-conjugated donkey anti-rabbit (Jackson ImmunoResearch Labs). Fixed and stained embryos were mounted in VectaShield (Vector Laboratories, Burlingame, CA) containing 0.5 μg/ml of DNA intercalating dye DAPI. At least 1000 embryos were examined for each experiment. Gonads were fixed and stained as in Howe *et al.* (2001). All images were captured on a Leica TCS NT microscope. Images of all embryos or gonads in Figures 3 and 4 are projections of four 0.5-μm sections.

RESULTS

Identification of the X signal element *ceh-39*: Previous analysis of duplications and deficiencies at the left end of X defined three distinct regions that harbor X signal elements, but only the XSE in region 3 (*fox-1*) was discovered (Figure 2A; Akerib and Meyer 1994; Hodgkin *et al.* 1994; Nicoll *et al.* 1997; Carmi and Meyer 1999). We designed an RNAi-based screen to identify ORFs in region 2 that function as XSEs (Figure 2, A and B). All 146 region 2 ORFs were assayed for XSE activity utilizing the sensitized strain *yDp14/yDp14* (X;I)*; him-8* IV*; fox-1* X, in which 94% of XO animals die from the increased dose of XSEs. The *fox-1* mutation sensitizes the screen to permit identification of weak XSEs. The homozygous *yDp14* duplication triples the dose of *fox-1*, the XSEs in region 2, and other potential XSEs adjacent to regions 2 and 3 (Akerib and Meyer 1994), causing XO animals to die from inappropriate repression of *xol-1* and the consequent reduction of X-linked gene expression (Table 1A). In principle, reducing the cumulative XSE activity in this strain by RNAi disruption of an XSE gene should increase the proportion of viable XO males, thus forming the basis for an efficient and sensitive assay to screen for XSE activity. An RNAi screen is more advantageous than a genetic screen, because RNAi reduces the activity of all copies of an XSE, whereas a mutation reduces only the activity of the single copy on X or on the duplication. Therefore, XSEs with even minor contributions to the signal should emerge from this screen. Our approach was validated by the observation that RNAi-mediated reduction of *fox-1* activity increased viability of *yDp14/yDp14; fox-1* males from 6 to 84% (Table 1A).

Of all 146 ORFs in region 2, only RNAi disruption of the gene corresponding to the ORF called T26C11.7 increased male viability significantly ($P \leq 0.01$), enhancing it to 84% and suggesting that T26C11.7 is an XSE (Table 1A). On average, RNAi against 13 random X ORFs not in region 2 or against 14 random ORFs on autosomes enhanced male viability to ~20%, a value not significantly different from the viability of *yDp14/yDp14; fox-1* males grown on bacteria containing the RNAi vector lacking a candidate gene (Table 1A). That the introduction of any dsRNA into the *yDp14/yDp14; fox-1* XO animals enhanced viability to this extent suggests that the RNAi machinery might affect dosage compensation, a topic currently under investigation (see Table 1, footnote *d*).

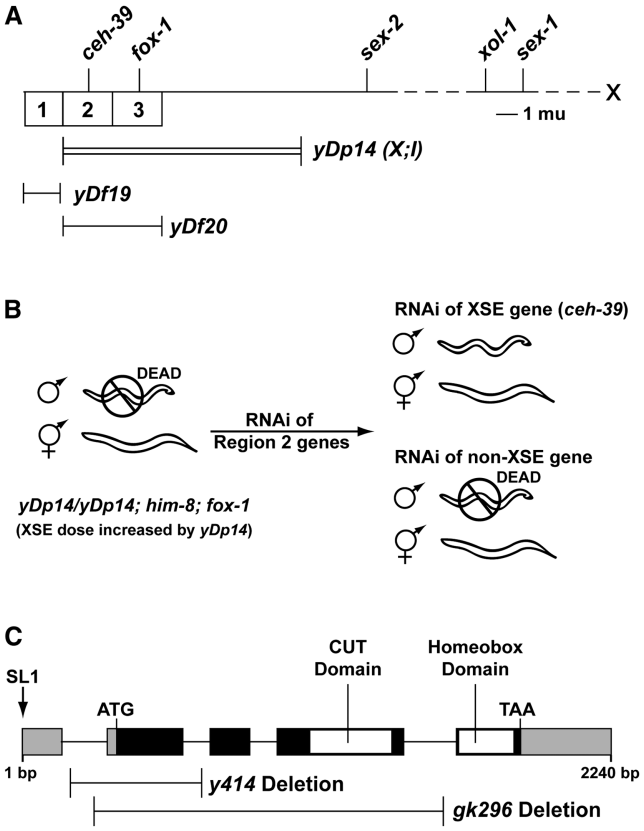

FIGURE 2.—Genetic map of the X chromosome, the RNAi-based screen for identifying XSEs in region 2, and the genomic region of *ceh-39*. (A) The X map highlights XSEs and *xol-1* (above the line) and three regions (numbered boxes) shown previously using duplications and deficiencies to contain X signal elements. The duplication *yDp14* covers region 2 (*ceh-39*) and region 3 (*fox-1*), the deficiency *yDf19* uncovers region 1, and the deficiency *yDf20* uncovers regions 2 and 3. (B) Screen for XSEs in region 2. The homozygous duplication *yDp14* increases XSE dose sufficiently in XO animals to repress *xol-1*, causing complete XO lethality. To identify potential XSEs, each ORF in region 2 was targeted for RNAi in *yDp14/yDp14; him-8; fox-1* animals, and their progeny were scored for the presence of males. Of all genes tested, only RNAi of *ceh-39* suppressed XO lethality, indicating that *ceh-39* is a potential XSE in region 2. (C) The genomic region spanning the *ceh-39* locus. Exons are indicated by solid boxes. The cut and homeobox domains are indicated by open boxes in the exons; 5′- and 3′-UTRs are indicated by shaded boxes. The arrow indicates where the SL1 *trans*-spliced leader is spliced to the 5′-UTR. ATG and TAA are the translational start and stop codons, respectively. The genomic region of *ceh-39* is 2240 bp, including introns, which are indicated by lines between the boxes. Locations of the two deletions in the *ceh-39* locus, *y414* and *gk296*, are indicated by single lines.

T26C11.7 represents the gene *ceh-39*, which encodes a member of the OC class of homeodomain proteins. The DNA-binding domain (DBD) of OC proteins is characterized by an atypical homeobox domain and a single cut domain. OC proteins mediate transcriptional regulation of numerous developmental processes (LANNOY *et al.* 1998). The discovery that an XSE in region 2 encodes a putative transcription factor came as somewhat of a surprise, since previous work suggested that region 2 likely contained a post-transcriptional regulator of *xol-1* (NICOLL *et al.* 1997). Experiments described below confirm that *ceh-39* regulates *xol-1* transcript levels and reconcile previous results.

C. elegans encodes five additional OC proteins, and the genes for two, *ceh-21* and *ceh-41*, reside on X in an operon with *ceh-39* (BLUMENTHAL *et al.* 2002; BURGLIN and CASSATA 2002). However, neither *ceh-21* nor *ceh-41* behaves like an XSE: RNAi against *ceh-21* or *ceh-41* increased the viability of *yDp14/yDp14; fox-1* XO animals to only 20 or 28%, respectively, levels comparable to the average levels achieved by RNAi against ORFs on autosomes or X chromosome ORFs not in region 2 (Table 1A). Moreover, simultaneous RNAi disruption of *ceh-21*, *ceh-41*, and *ceh-39* did not further increase the viability of *yDp14/yDp14; fox-1* XO animals (Table 1A). Thus, XSE activity is specifically a property of *ceh-39* and not of other X-linked OC genes.

To characterize *ceh-39* genetically, two *ceh-39* mutants were isolated (Figure 2C; see MATERIALS AND METHODS). *ceh-39(y414)* deletes part of the *ceh-39* locus, resulting in a conceptual protein that lacks the first 102 amino acids but retains both the homeobox and cut domains. The allele *ceh-39(gk296)* is a larger deletion that eliminates the N terminus and the cut domain. XX and XO animals carrying either mutation have a wild-type phenotype (Table 3 and data not shown). Both mutations synergize with a *fox-1* mutation to suppress all the male lethality caused by one copy of *yDp14*, providing genetic confirmation that the *ceh-39* locus behaves like an XSE (Table 1B).

***ceh-39* and *fox-1* are not the only XSEs in the *yDp14* interval:** If *ceh-39* and *fox-1* were the only significant contributors to the cumulative XSE dose in *yDp14*, then the *ceh-39 fox-1* double mutations should rescue all *yDp14/+* males and restore the viability of *yDp14/yDp14* males to that of *yDp14/+* males. All *yDp14/+; ceh-39(y414 or gk296) fox-1* males appeared viable (Table 1B). However, the viability of *yDp14/yDp14*; *ceh-39 fox-1* XO animals was only ~2–13% of the viability of *yDp14/+* XO animals. Thus, *ceh-39* and *fox-1* are important XSEs in the interval of X represented by *yDp14*, but they are not the only XSEs. This duplicated region extends beyond region 3 by 7 MU (including >450 ORFs), suggesting that additional XSEs reside in this region of X.

***ceh-39* acts upstream of *xol-1*:** If *ceh-39* is a *bona fide* XSE, it should exert its effect on dosage compensation by repressing *xol-1*, rather than a downstream gene in the dosage compensation pathway. In XX animals, mutations in XSEs derepress *xol-1*, causing disruption of dosage compensation and the consequent XX-specific phenotypes, including lethality, an egg-laying defect (Egl), and dumpy (Dpy) morphology, all of which are suppressed by a *xol-1* mutation (AKERIB and MEYER 1994; CARMI *et al.* 1998). Although *ceh-39* mutations by themselves cause no obvious dosage compensation phenotype in XX mutants, they enhance the XX-specific

TABLE 1

***ceh-39* is an XSE in region 2**

yDp14/yDp14; him-8; fox-1 XO + RNAi of gene[a]	Male viability (%)[b]	*n*[c]
A. RNAi of *ceh-39* suppresses the XO-specific lethality caused by the increase in XSE dose from two copies of *yDp14*		
No RNAi vector or gene	6	1225
RNAi vector with no gene	18[d]	1236
fox-1(RNAi)	84[d]	1050
ceh-39(RNAi)	84[d]	857
ceh-21(RNAi)	20[d]	776
ceh-41(RNAi)	28[d]	923
ceh-39(RNAi), *ceh-21*(RNAi), *ceh-41*(RNAi)	76[e]	946
RNAi of X ORFs not in region 2	19 ± 9[f] (13 genes)	NA
RNAi of ORFs on autosomes	18 ± 7[f] (14 genes)	NA

XO genotype[g]	*ceh-39* and *fox-1* dose	Male viability (%)	*n*[c]
B. *ceh-39* and *fox-1* are not the only XSEs in *yDp14*			
Wild type[h]	1	100	1632
yDp14/+[i]	2	61	724
yDp14/+; ceh-39(y414) fox-1(y303)[j]	1	98	1369
yDp14/+; ceh-39(gk296) fox-1(y303)[j]	1	102	1566
yDp14/yDp14; him-8(e1489)[k]	3	0	929
yDp14/yDp14; *ceh-39(y414) fox-1(y303)*[k]	2	8	863
yDp14/yDp14; *ceh-39(gk296) fox-1(y303)*[k]	2	1	716

[a] Candidate genes were tested for XSE activity. *yDp14/yDp14(X;I); him-8(e1489) IV; dpy-3(e27) fox-1(y303) unc-2(e55)* X hermaphrodites were treated with RNAi against the indicated gene, and the viability of progeny males was assessed. In all cases except as described in footnote *e*, the RNAi was achieved through feeding. RNAi-mediated knockdown of an XSE should decrease the male lethality caused by the increase in XSE dose from *yDp14*. Animals were fed bacteria that produced dsRNA to the listed gene (see MATERIALS AND METHODS). *yDp14* is an X duplication attached to LG I and can exist in one copy (*yDp14/+*) or two copies (*yDp14/yDp14*) (AKERIB and MEYER 1994). *him-8* XX animals produce 37% XO males, 57% XX hermaphrodites, and 6% Dpy XXX hermaphrodites (HODGKIN *et al.* 1979).

[b] Male viability was calculated by the following formula: (no. of adult males)/(expected no. of males) × 100. The number of expected males was (0.37) *n*.

[c] *n* is the total number of embryos from six independent sets of progeny counts.

[d] Male viability is significantly higher only for *fox-1*(RNAi) and *ceh-39*(RNAi), both $P \leq 0.01$, when compared to male viability of the true control: *yDp14/yDp14; him-8; fox-1* animals grown on bacteria carrying an RNAi vector with no gene insert. Male viability for neither *ceh-21*(RNAi) ($P = 0.70$) nor *ceh-41*(RNAi) ($P = 0.02$) was significantly different from the true control. Male viability due to RNAi of these genes instead was equivalent to that due to RNAi of random X ORFs not in region 2 or of autosomal ORFs. The unexpected observation that RNAi against any *C. elegans* gene, or even the introduction of double-stranded RNA not similar to *C. elegans* RNA, rescued some XO lethality caused by *yDp14/yDp14* suggests that the RNAi machinery may affect the sex-determination and dosage compensation pathway. This RNAi effect appears to be weak since it was observed only in the sensitized XO genetic background and only when RNAi was achieved through dsRNA feeding. Induction of RNAi in XX animals did not cause a notable dosage compensation disruption, and thus the observed effects of RNAi in XX animals (Table 3) are due to the reduced function of the XSE genes targeted.

[e] RNAi was achieved by simultaneously injecting double-stranded RNA from *ceh-39*, *ceh-21*, and *ceh-41*. Injection RNAi against *fox-1* resulted in 87% male viability ($n = 1217$); against *ceh-39*, 85% male viability ($n = 759$); and against dsRNA made from the vector with no cloned gene, 6% male viability ($n = 1002$).

[f] The numbers presented include the average and the standard deviation of male viability for RNAi against 13 X ORFs not in region 2 (C05D9.5, F49E7.1, C05D9.7, R193.2, R193.3, R193.1, T13G4.3, F09E10.3, F09E10.6, F09E10.7, F09E10.8, K06A9.1, K06A9.2) and 14 ORFs on autosomes (F44E8.2, C31H1.1, C31H1.2, C31H1.5, C31H1.6, C31H1.7, C31H1.8, C10G6.1, T10B9.3, T10B9.4, T10B9.5, T10B9.7, T10B9.8, ZK938.1). Approximately 200 embryos were scored per ORF tested.

[g] These animals also carry a *dpy-3(e27)* mutation, except for *yDp14/+* and *yDp14/yDp14; him-8(e1489)* animals, which carry *unc-2(e55)* instead.

[h] Males were generated by mating wild-type males and hermaphrodites. Male viability was calculated by the following formula: [adult males]/[expected no. of males, (0.5) *n*] × 100. The number of hermaphrodites was 0.5(*n*), implying a viability of 100% and a mating that produced only cross progeny.

[i] Males were produced by mating wild-type males with *yDp14/yDp14; unc-2(e55)* hermaphrodites. The number of hermaphrodites was (0.5) *n*, indicating that the hermaphrodite viability was 100% and the cross went to completion.

[j] *yDp14/+; ceh-39 fox-1* males were generated from a cross of *mIs11* males with *yDp14/yDp14; ceh-39 fox-1* hermaphrodites. *mIs11* is a dominant, integrated transgenic marker that expresses GFP from pes-10 and myo-2 promoters and a gut-specific enhancer. It was used to identify cross progeny. Male viability was calculated by the following formula: [adult males)]/[expected no. of males, (0.5) *n*] × 100. All progeny were *gfp*(+), indicating that the cross went to completion.

[k] *yDp14/yDp14; mIs11/+; ceh-39(y414* or *gk296) fox-1(y303)* males were generated by crossing *yDp14/+; mIs11*; *ceh-39(y414* or *gk296) fox-1(y303)* males with *yDp14/yDp14; ceh-39(y414* or *gk296) fox-1(y303)* hermaphrodites. Fifty percent of the XO (male) cross progeny should be of genotype *yDp14/yDp14; ceh-39(y414* or *gk296) fox-1(y303)*. Since another 50% of the XO progeny are *yDp14/+; ceh-39(y414* or *gk296) fox-1(y303)*, which are ~100% viable, the viability of *yDp14/yDp14; ceh-39(y414* or *gk296) fox-1(y303)* XO males was calculated by the following formula: [no. of males − (0.25) *n*]/[expected no. of *yDp14/+* males, (0.25) *n*] × 100.

TABLE 2

ceh-39* acts upstream of *xol-1

Genotype[a]	Hermaphrodite viability (%)[b]	*n*[c]
ceh-39(y414)	101	1008
xol-1(y9)[d]	97	1251
ceh-39(y414) xol-1(y9)[d]	93	1120
dpy-27(y57)	77	1164
dpy-27(y57); xol-1(y9)	77	1435
dpy-27(y57); ceh-39(y414)	18	1130
dpy-27(y57); xol-1(y9) ceh-39(y414)[d]	70	964
sdc-2(RNAi)	84	1512
xol-1(y9) sdc-2(RNAi)[d]	84	722
ceh-39(y414) sdc-2(RNAi)	53	1157
ceh-39(y414) xol-1(y9) sdc-2(RNAi)[d]	89	1416

[a] RNAi was applied as explained in Table 1, footnote *a*.
[b] Hermaphrodite viability was calculated by the following formula: (no. of adult hermaphrodites)/(total no. of embryos) × 100.
[c] *n* is the total number of embryos from six independent sets of progeny counts.
[d] Strain also includes the marker *dpy-6(e14)*.

lethality caused by hypomorphic mutations in dosage compensation genes such as *dpy-27* or *sdc-2*, which act downstream of *xol-1* (Figure 1). If *ceh-39* acts through *xol-1*, then a *xol-1* mutation should suppress the synergistic XX lethality caused by the combination of *dpy-27* and *ceh-39* mutations or *ceh-39* and *sdc-2* mutations. Moreover, the triple-mutant XX animals (*dpy-27; ceh-39 xol-1* or *ceh-39 xol-1 sdc-2*) should have the same phenotypes as either *dpy-27* or *sdc-2* single mutants, respectively.

The hypomorphic *dpy-27(y57)* mutation reduced XX viability to 77% (Table 2; Plenefisch *et al.* 1989), and the *dpy-27; ceh-39(y414)* double combination further reduced XX viability to 18%; survivors had more severe Dpy and Egl phenotypes. The synergistic XX lethality was almost completely suppressed by a *xol-1* null mutation: ~70% of *dpy-27; ceh-39 xol-1* XX animals were viable, indicating that *ceh-39* functions upstream of *xol-1* to repress it (Table 2). The synergistic lethality between *ceh-39(y414)* and *sdc-2*(RNAi) was also suppressed by a *xol-1* mutation (Table 2), further confirming that *ceh-39* controls *xol-1* either directly or indirectly.

Criteria for an X signal element: The hallmark of an X signal element is that changing its dose causes reciprocal effects on the viability of XX and XO animals. First, decreasing XSE dose selectively kills XX animals by activating *xol-1* and thereby inhibiting the dosage compensation machinery. Second, increasing XSE dose selectively kills XO animals by repressing *xol-1* and thereby activating the dosage compensation machinery. XSEs act cumulatively such that increasing or decreasing the dose of multiple XSEs affects viability more severely than changing the dose of a single XSE. Third, increasing the dose of one XSE in XX animals compensates for decreasing the dose of a different XSE, and decreasing the dose of one XSE in XO animals compensates for increasing the dose of another. The compensating changes restore the cumulative XSE signal to a level approaching that of the wild-type signal. Fourth, an XSE acts in a dose-dependent manner in the zygote, since the zygotic X:A signal determines sex. Results described in the sections below show that *ceh-39* meets these criteria and therefore acts as an X signal element in promoting the hermaphrodite fate.

Decreasing *ceh-39* dose enhances the XX lethality caused by reduced XSE dose: Mutations in individual XSEs have small-to-moderate effects on XX animals, but mutations in multiple XSEs can cause pronounced dosage compensation defects and extensive XX-specific lethality (Table 3; Carmi and Meyer 1999). For example, 70% of hypomorphic *sex-1* XX mutants are viable, and virtually all *fox-1* XX or *sex-2* XX single mutants are viable, but nearly all *fox-1 sex-1* or *sex-2 sex-1* XX double mutants are dead ($P < 0.01$; Table 3); Carmi *et al.* 1998). Similarly, decreasing *ceh-39* dose enhances the XX lethality caused by loss of other XSEs. While neither *ceh*-39 RNAi nor a *ceh-39* mutation causes visible phenotypes, both cause nearly complete XX lethality (10 and 7%, respectively) in combination with a *sex-1* hypomorphic mutation ($P < 0.01$; Table 3). This effect is XX specific: all *ceh-39 sex-1* XO double mutants are viable (data not shown). In contrast, RNAi of *ceh-21* did not enhance the lethality of *sex-1* XX mutants (Table 3), demonstrating that synergistic lethality is not a general property of OC gene disruptions and that the general process of RNAi does not demonstrably affect the X signal in XX animals.

ceh-39 and *fox-1* are relatively weak XSEs, but even weak XSEs make important contributions to the X signal (Table 3). *ceh-39* XX, *fox-1* XX, or *sex-2* XX mutants are wild type. However, *ceh-39 fox-1* XX double mutants are mildly Dpy in phenotype (Table 3), as are *ceh-39*(RNAi) *sex-2* XX double mutants and *fox-1 sex-2* XX double mutants, suggesting that *ceh-39* and *fox-1* make similar contributions to the X signal. The triple-mutant combination *ceh-39 fox-1 sex-2* caused slightly more Dpy and Egl phenotypes than double-mutant combinations and a slight reduction in viability (92% viable, $P < 0.01$) compared to double mutants (98–100% viable), further illustrating the cumulative action of XSEs.

Decreasing the dose of *ceh-39* and other XSEs disrupts the DCC in XX animals: The extent of XX-specific lethality caused by mutations in one or more XSEs was found to be well correlated with the degree of disruption in the dosage compensation complex (Figure 3, A–J). In wild-type XX animals, the dosage compensation complex assembles on both X chromosomes to reduce transcript levels by half (Chuang *et al.* 1994; Lieb *et al.* 1996, 1998; Davis and Meyer 1997; Dawes *et al.* 1999; Chu *et al.* 2002). Consistent with the full viability and wild-type appearance of *fox-1* XX or *ceh*-39 XX mutants, the DCC proteins DPY-27 (Figure 3, A and a; E and e; G

TABLE 3

***ceh-39* mutations enhance XX-specific phenotypes caused by other XSE mutations**

Genotype[a]	Survivor phenotype	Hermaphrodite viability (%)[b]	*n*[c]
ceh-39(y414)	Wild type	101	1008
ceh-39(gk296)	Wild type	102	1021
ceh-39(RNAi)	Wild type	100	807
ceh-21(RNAi)	Wild type	100	1147
fox-1(y303)	Wild type	99	1054
sex-2(y324)	Wild type to mild Dpy	99	1032
sex-1(y263)	Dpy, Egl Tra	70	884
sex-1(RNAi)	Very Dpy, Egl, Tra	17	1090
sex-1(y263, RNAi*)*	Very Dpy, Egl, Tra	17	1304
sex-2(y324) sex-1(y263)[d]	Very Dpy	4	238
fox-1(y303) sex-1(y263)[e]	Very Dpy, Egl, Tra	4	1176
fox-1(y303) sex-1(RNAi)	Very Dpy, Egl, Tra	9	749
ceh-39(y414) sex-1(y263)[f]	Very Dpy, Egl, Tra	7	982
ceh-39(y414) sex-1(y263)[e]	Very Dpy, Egl, Tra	5	941
ceh-39(RNAi) *sex-1(y263)*	Very Dpy, Egl	10	832
ceh-39(y414) sex-1(RNAi)	Dead	0	935
ceh-39(gk296) sex-1(RNAi)	Dead	0	1637
ceh-21(RNAi) *sex-1(y263)*	Dpy, Egl	75	1043
ceh-39(y414) fox-1(RNAi)	Mild Dpy	98	1486
ceh-39(gk296) fox-1(RNAi)	Mild Dpy	101	1256
ceh-39(RNAi) *fox-1(y303)*	Mild Dpy	100	729
ceh-39(RNAi) *sex-2(y324)*	Dpy, Egl	99 ± 2[g]	1368
fox-1(y303) sex-2(y324)	Dpy, Egl	98 ± 1[g]	1010
ceh-39(RNAi) *fox-1(y303) sex-2(y324)*	Dpy, Egl	92 ± 1[g]	1180

[a] RNAi was applied as explained in Table 1, footnote *a*.

[b] Hermaphrodite viability was calculated by the following formula: (no. of adult hermaphrodites)/(total no. of embryos) × 100.

[c] *n* is the total number of embryos from six independent sets of progeny counts.

[d] Data are from C. Y. Loh and B. J. Meyer (personal communication). Of 951 progeny from *sex-2(y324) sex-1(y263)/szT1* animals, only 9 (of an expected 238) lacked *szT1*, implying that they were *sex-2(y324) sex-1(y263)* and only 4% were viable. *sex-2(y324) sex-1(y263)* animals were severely Dpy and produced no or few progeny.

[e] Percentage viability of *fox-1(y303) sex-1(y263)* XX progeny from the strain *fox-1(y303) sex-1(y263)/szT1* and percentage viability of *ceh-39(y414) sex-1(y263)* XX progeny from the strain *ceh-39(y414) sex-1(y263)/szT1* were calculated by the following formula: (no. of Dpy hermaphrodites)/0.25(*n* − no. of males) × 100. The *szT1* balancer acts as a mild dominant *him* mutation, making it necessary to calculate the expected number of XX adults by subtracting the number of XO male progeny from the total number of embryos.

[f] This strain is maintained under *yEx483[dpy-30::sdc-2(+); myo-2::gfp(+)]*, an extrachromosomal array that rescues XSE mutants because it overexpresses *sdc-2*. To score viability, progeny from *gfp*(−) hermaphrodites that had lost *yEx483* were counted.

[g] Viability was calculated separately for six independent sets of progeny counts. Average viability and error are reported. Error is expressed as the standard error of the mean.

and g; I and i) and SDC-3 (data not shown) exhibited a wild-type X-localized pattern. The DCC was only mildly disrupted in *sex-1* hypomorphic mutants (70% viable) (Figure 3, C and c) and more severely disrupted in *sex-1*(RNAi) XX animals (Figure 3, B and b) or *sex-1(y263,* RNAi*)* XX mutants (Figure 3, D and d), both of which were ~17% viable. In the latter two cases, DPY-27 and SDC-3 (data not shown) appeared punctate in many nuclei and diffuse or absent in others. The most dramatic disruption of the DCC was evident in *fox-1 sex-1* (RNAi) embryos (Figure 3, F and f) and *ceh-39 sex-1* (RNAi) embryos (Figure 3, H and h; J and j), all of which were inviable. Most nuclei had very little or no DPY-27 or SDC-3 (data not shown) protein, and the residual protein had either a diffuse nuclear or punctate appearance. This dramatic reduction in DCC levels suggests that the complete lethality observed in these double mutants is due to a disruption in dosage compensation.

Increasing *ceh-39* dose enhances the XO lethality caused by increased XSE dose: Increasing the dose of *ceh-39* using *yIs58[ceh-39(+)]*, an integrated array bearing multiple copies of the 5.5-kbp genomic fragment spanning *ceh-39*, caused no XO lethality by itself but enhanced the lethality caused by one copy of *yDp14*, which duplicates *ceh-39*, *fox-1*, and other not-yet-identified XSEs (Table 4). One copy of *yIs58[ceh-39(+)]* reduced the viability of *yDp14/+* XO males from 61 to 20% ($P < 0.01$). Two copies of *yIs58[ceh-39(+)]*, shown to increase the *ceh-39* transcript level fourfold above that of the wild-type level (Gladden *et al.* 2007, accompanying article in

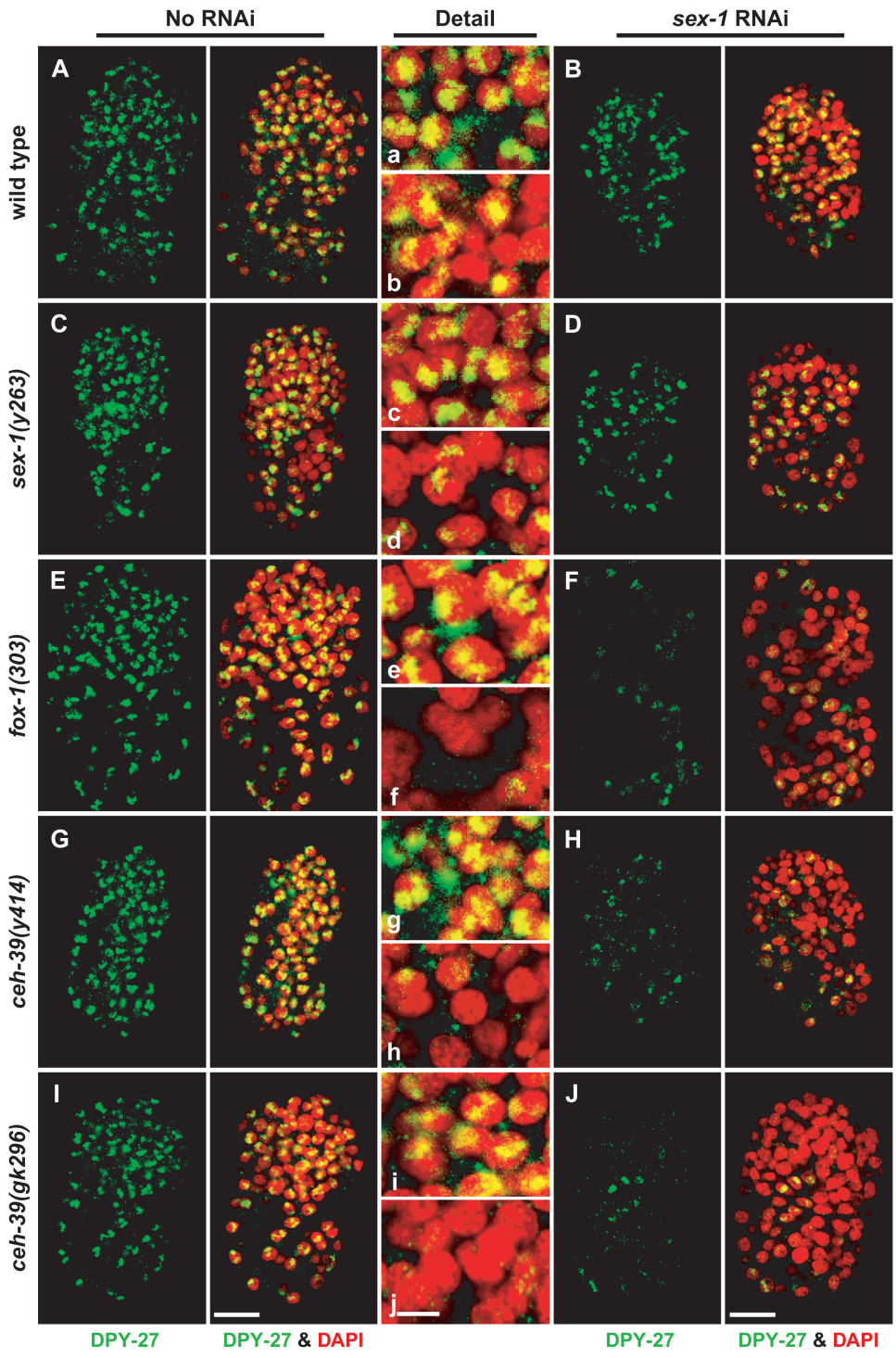

FIGURE 3.—Decreasing the dose of *ceh-39* and other XSEs disrupts the dosage compensation complex in XX animals. Localization of DPY-27 in wild-type and XSE mutant embryos with and without RNAi disruption of *sex-1*. (A–J) Partial projections of false-colored confocal images of wild-type and mutant XX embryos costained with antibodies against DPY-27 (green) and the DNA intercalating dye DAPI (red). (a–j) Enlargements of nuclei from A–J, respectively. (A, E, G, and I) DPY-27 localized in a punctate pattern to the X chromosomes of wild-type XX embryos, and *fox-1* or *ceh-39* mutant XX embryos. (C) The *sex-1(y263)* mutant embryos exhibited a reduction in DPY-27 staining. Some nuclei showed sparse or no staining and others varied from punctate to diffuse staining, all implying less DPY-27 on X. (B and D) *sex-1*(RNAi) XX embryos and *sex-1*(*y263*, RNAi) mutants showed a further decrease in DPY-27 signal compared to that in *sex-1* mutants. The residual DPY-27 was mostly punctate, indicating X localization. (F, H, and J) The DPY-27 signal was drastically reduced in *fox-1 sex*-1(RNAi) XX and *ceh-39 sex*-1(RNAi) XX mutants; the small quantity of residual DPY-27 had punctate localization. The more severe reduction in DPY-27 signal after knockdown of two XSEs rather than one shows that dosage compensation is disrupted more in double than in single XSE mutants, as is viability. In the images, DPY-27 signal was enhanced in all embryos treated with RNAi of *sex-1* to demonstrate the punctate localization more clearly. Bars: A–J, 10 μm; a–j, 3 μm.

this issue), further reduced viability of *yDp14*/+ males to 3%, suggesting that *ceh-39* represses *xol-1* in a dose-dependent manner, another characteristic of XSEs ($P < 0.01$ for viability of *yIs58*/+ *vs. yIs58*/*yIs58* XO animals).

Changes in *ceh-39* dose compensate for reciprocal changes in the dose of other XSEs: The screen used to identify *ceh-39* demonstrated that decreasing the dose of *ceh-39* suppressed the XO-specific lethality caused by elevated XSE dose in *yDp14/yDp14; fox-1* animals (Table 1). Reciprocal suppression also occurred: increasing *ceh-39* dose suppressed the XX-specific lethality caused by all combinations of single and double XSE mutations tested (Table 5). Two copies of *yIs58*[*ceh-39*(+)] increased the viability of *sex-1* XX mutants from 70 to 98%, *fox-1 sex-1* mutants from 0 to 76%, and *sex-2 sex-1* mutants from 4 to 69% ($P < 0.01$ for all pairwise comparisons). The rescued XX mutants were Dpy, indicating lingering dosage compensation defects despite high viability. This

TABLE 4

Increased dose of *ceh-39* enhances XO-specific lethality caused by increased XSE dose

XO genotypes	No. of males	Male viability (%)[a]	n[b]
Wild type[c]	812	100	1632
yIs58[*ceh-39(+)*]/*yIs58*[d]	555	98	1131
yDp14/+[e]	220	61	724
yDp14/+; yIs58[*ceh-39(+)*]*/+*[f]	141	20	1440
yDp14/+; yIs58[*ceh-39(+)*]*/yIs58*[g]	22	3	1522

[a] Males were generated through crosses and their viability was calculated by the following formula: [no. of adult males]/[the expected no. of males, $(0.5)n$] × 100. In all crosses, the number of hermaphrodites was $0.5(n)$, implying that the matings produced only cross progeny and that hermaphrodite viability was 100%.

[b] n is the total number of embryos from six independent sets of progeny counts.

[c] Wild-type males were produced by mating wild-type males and hermaphrodites.

[d] Males were produced by mating *yIs58*[*ceh-39(+)*]*/yIs58* males and hermaphrodites. *yIs58*[*ceh-39(+)*] is an integrated transgenic array carrying multiple copies of a 5.5-kbp genomic fragment spanning the entire *ceh-39* locus. Two copies of *yIs58* elevate the *ceh-39* transcript level fourfold above the wild-type level (Gladden *et al.* 2007, accompanying article in this issue).

[e] Males were produced by mating wild-type males with *yDp14/yDp14; unc-2(e55)* hermaphrodites.

[f] Males were generated by mating *yIs58*[*ceh-39(+)*]*/yIs58* males with *yDp14/yDp14; unc-2(e55)* hermaphrodites.

[g] Males were generated by mating *yIs58*[*ceh-39(+)*]*/yIs58* males with *yDp14/yDp14; yIs58/yIs58; unc-2(e55)* hermaphrodites.

TABLE 5

Overexpression of *ceh-39* rescues XX-specific lethality caused by disruption of other XSE genes

Genotype[a]	Hermaphrodite viability (%)[b]	n[c]
sex-1(y263)	70	884
sex-1(y263); yIs58[*ceh-39(+)*]*/ yIs58*[*ceh-39(+)*][d]	98	1399
sex-1(y263, RNAi*)*	17	1304
sex-1(y263, RNAi*); yIs58/yIs58*	71	597
fox-1(y303) sex-1(y263)	4	1176
fox-1(y303) sex-1(y263); yIs58/yIs58	76	784
sex-2(y324) sex-1(y263)[e]	4	238
sex-2(y324) sex-1(y263); yIs58/yIs58	69	1286
ceh-39(RNAi) *sex-1(y263); yIs58/yIs58*[f]	5	440
ceh-39(RNAi) *fox-1(y303) sex-1(y263); yIs58/yIs58*[f]	0	480

[a] RNAi was applied as explained in Table 1, footnote *a*.

[b] Hermaphrodite viability was calculated by the following formula: (no. of adult hermaphrodites)/(total no. of embryos) × 100.

[c] n is the total number of embryos from six independent sets of progeny counts.

[d] *yIs58*[*ceh-39(+)*] is an integrated transgene consisting of multiple copies of a 5.5-kbp genomic fragment spanning the *ceh-39* locus.

[e] Data are from C. Y. Loh and B. J. Meyer (personal communication). See footnote *d* in Table 3.

[f] The rescue of XSE mutants is specific to increased *ceh-39* dose because RNAi of *ceh-39* not only abolished the suppression caused by *yIs58*, but also reduced the activity of *ceh-39* completely, causing synergistic lethality in combination with XSE mutations.

rescue was specific to *ceh-39*, since *ceh-39* RNAi not only abolished the ability of *yIs58*[*ceh-39(+)*] to rescue XSE mutants, but also actually caused synergistic lethality in single and double XSE mutants (Table 5). Thus, increasing *ceh-39* dose can compensate for a decreased dose of other XSEs, thereby restoring the X signal and repressing *xol-1*.

***ceh-39* acts in the zygote:** Sex is specified by the X chromosome dose of the zygote. Thus, for *ceh-39* to be classified as an XSE, changing the dose of *ceh-39* in the zygote should perturb viability. In the previously described experiments showing that increasing *ceh-39* dose adversely affected XO animals, the increased *ceh-39* dose from one copy of *yIs58*[*ceh-39(+)*] in *yDp14/+* XO males was supplied paternally, indicating that the increase in XO lethality resulted from a change in zygotic activity of *ceh-39*. Thus, *ceh-39* meets the fourth and final criterion for an XSE.

***ceh-39* does not regulate known XSEs or the ASE *sea-1*:** The results presented thus far show that *ceh-39* acts as an XSE to repress *xol-1*. *ceh-39* could function by activating another XSE by repressing an activator of *xol-1* such as an ASE or by acting directly on *xol-1*. If *ceh-39* activates a single known XSE, then mutation of both should cause the same degree of *xol-1* derepression as loss of just the downstream XSE, provided the downstream XSE mutation is a null. Instead, loss of *ceh-39* activity causes synergistic XX-specific dosage compensation phenotypes in combination with null mutations (or RNAi) of XSEs, making it unlikely that *ceh-39* acts through them (Table 3). Reinforcing this conclusion is the fact that increasing the *ceh-39* dose rescues all known XSE mutants (Table 5).

If *ceh-39* represses a specific ASE, then mutation of *ceh-39* should increase expression of the target ASE gene and thereby hyperactivate *xol-1* in an XX embryo, causing a dosage compensation disruption. Mutation of the target ASE would suppress the *ceh-39* mutation by preventing the upregulation of *xol-1* expression. This scenario was not found for the ASE *sea-1*. *sea-1* activates *xol-1* expression, and a *sea-1* mutation rescues 57% of *fox-1 sex-1* mutants by reducing *xol-1* activation (Table 6; Powell *et al.* 2005). If *ceh-39* were a repressor of *sea-1*, then a *sea-1* mutation would block the complete synergistic XX lethality between *ceh-39* RNAi and *fox-1 sex-1* mutations. Instead, if *ceh-39* acts independently of *sea-1*, then *ceh-39* RNAi should reduce the viability of *fox-1 sex-1* mutants even in the presence of a *sea-1* mutation. Indeed, *ceh-39*

TABLE 6

An autosomal signal element mutation cannot suppress loss of three XSEs

Genotype[a]	Hermaphrodite viability (%)[b]	*n*[c]
sea-1(y356); fox-1(y303) sex-1(y263)	57	1054
sea-1(y356); fox-1(y303) sex-1(y263) ceh-39(RNAi)	0	2016

[a] RNAi was applied as explained in Table 1, footnote *a*.
[b] Hermaphrodite viability was calculated by the following formula: (no. of adult hermaphrodites)/(total no. of embryos) × 100.
[c] *n* is the total number of embryos from six independent sets of progeny counts.

RNAi did reduce the viability of *sea-1; fox-1 sex-1* XX mutants from 57 to 0% ($P < 0.01$; Table 6). Therefore, *ceh-39* appears not to act through *sea-1*.

Furthermore, *ceh-39* is unlikely to be the exclusive regulator of any ASE. If *ceh-39* were the sole and complete repressor of a single ASE, the *ceh-39* dose should be sufficiently high in XX animals to repress the ASE. If this were the case, increasing *ceh-39* dose in XX animals should not alleviate *xol-1* derepression caused by mutations in other XSEs, since its target ASE would already be repressed. However, increasing *ceh-39* dose strongly suppresses single and double XSE mutants (Table 5). Together, the results suggest that *ceh-39* acts as a direct repressor of *xol-1* or functions as an activator of an undefined XSE.

CEH-39 accumulates in a spatial and temporal pattern appropriate for an XSE: The expression patterns of known XSEs match the time window in which *xol-1* repression is critical: during gastrulation from the ~28- to 350-cell stage (Rhind *et al.* 1995; Nicoll *et al.* 1997; Carmi *et al.* 1998). To assess whether CEH-39 accumulation is consistent with its role as an XSE, we raised an antibody against CEH-39 and examined its immuno-localization in wild-type and *ceh-39* mutant animals. In wild-type embryos, CEH-39 was first detectable in the 2-cell stage, but robust CEH-39 accumulation began at the 8-cell stage and tapered off by the 150-cell stage, disappearing almost completely by the 200-cell stage (Figure 4, A–C), consistent with a role in repressing *xol-1*. No antibody staining was detected in *ceh-39* mutants, confirming antibody specificity (Figure 4D). CEH-39 also appeared to associate with condensed DNA. During mitosis, CEH-39 was detected on metaphase and anaphase chromosomes (Figure 4A). However, no obvious mitotic defects were found in *ceh-39* mutants, suggesting that the accumulation of this OC protein on condensed DNA may simply reflect a nonspecific affinity for DNA or a minor function in mitosis. The presence of CEH-39 in 2-cell embryos and also in hermaphrodite gonads (Figure 4, E and F) correlates with a previous study showing that the XSE in region 2, the location of *ceh-39*, has a maternal component (Carmi and Meyer 1999). In the gonad, CEH-39 nuclear staining was observed from late pachytene through diakinesis. Staining colocalized with the condensed diakinetic chromosomes.

***ceh-39* requires sequences in the *xol-1* coding region to repress it:** The identification of CEH-39 as a OC transcription factor suggested that CEH-39 would regulate *xol-1* transcript levels. However, previous studies suggested that the XSE in region 2 did not act on a transcriptional level (Carmi *et al.* 1998). In XX animals, a heterozygous deficiency that uncovers region 2 and *fox-1* (*yDf20*) failed to derepress a *xol-1* transcriptional *Pxol-1::lacZ* reporter transgene (*yIs33*), in which *lacZ* expression was controlled by the 2.8-kbp *xol-1* promoter. In contrast, both a *sex-1* mutation and a heterozygous deficiency that uncovers region 1 (*yDf19*) caused robust derepression of *yIs33* (Figure 2A; Figure 5, A and D; Nicoll *et al.* 1997; Carmi *et al.* 1998). Thus, *fox-1* and the XSE in region 2 appeared to repress *xol-1* post-transcriptionally, while the XSE in region 1 and *sex-1* appeared to repress *xol-1* transcriptionally. This interpretation was reinforced by finding that *yIs33* was also not derepressed in the *ceh-39(y414)* deletion mutant (Figure 5D). However, these results did not preclude the possibility that *ceh-39* might regulate *xol-1* transcript levels through sites not present in the *yIs33* reporter.

To examine the regulation of *xol-1* by *ceh-39* more extensively, a reporter transgene encompassing a larger genomic region of *xol-1* was analyzed. Results from these experiments indicate that *ceh-39* represses *xol-1* through sequences present in the *xol-1*-coding region. In this reporter, the *lacZ* gene is under the control of a genomic fragment spanning the 2.8-kbp *xol-1* promoter and the first three exons (*yIs2*, *xol-1::lacZ*) (Figure 5B). Both *sex-1*, and to a lesser extent, *ceh-39* mutations derepress *yIs2*. Homozygous *sex-1(y263)* and *ceh-39(y414)* mutations caused 67 and 42%, respectively, of *yIs2* XX hermaphrodites to produce embryos expressing high levels of *lacZ* compared to only 3% of *yIs2* XX control hermaphrodites ($P < 0.01$; Figure 5D). These results show that loss of *ceh-39* alone is sufficient to derepress *xol-1*. The fact that the *ceh-39* mutation causes less derepression of *yIs2* than the *sex-1* mutation suggests that *ceh-39* is a weaker repressor of *xol-1* than *sex-1*, consistent with the weaker phenotypes of *ceh-39* mutants.

Because *ceh-39* is a *xol-1* repressor, increasing the *ceh-39* dose should counteract the derepression of *xol-1* caused by the loss of another XSE such as *sex-1*. In fact, increasing *ceh-39* dose using the integrated transgene *yIs58*[*ceh-39(+)*] reduced the extent of *yIs2* derepression caused by a *sex-1* mutation (Figure 5, C and D). Only 26% of *yIs2; yIs58/yIs58; sex-1(y263)* XX hermaphrodites produced embryos expressing high levels of *lacZ*, in contrast to 67% of *yIs2; sex-1(y263)* hermaphrodites ($P < 0.01$). Furthermore, the increase in *ceh-39* dose had no

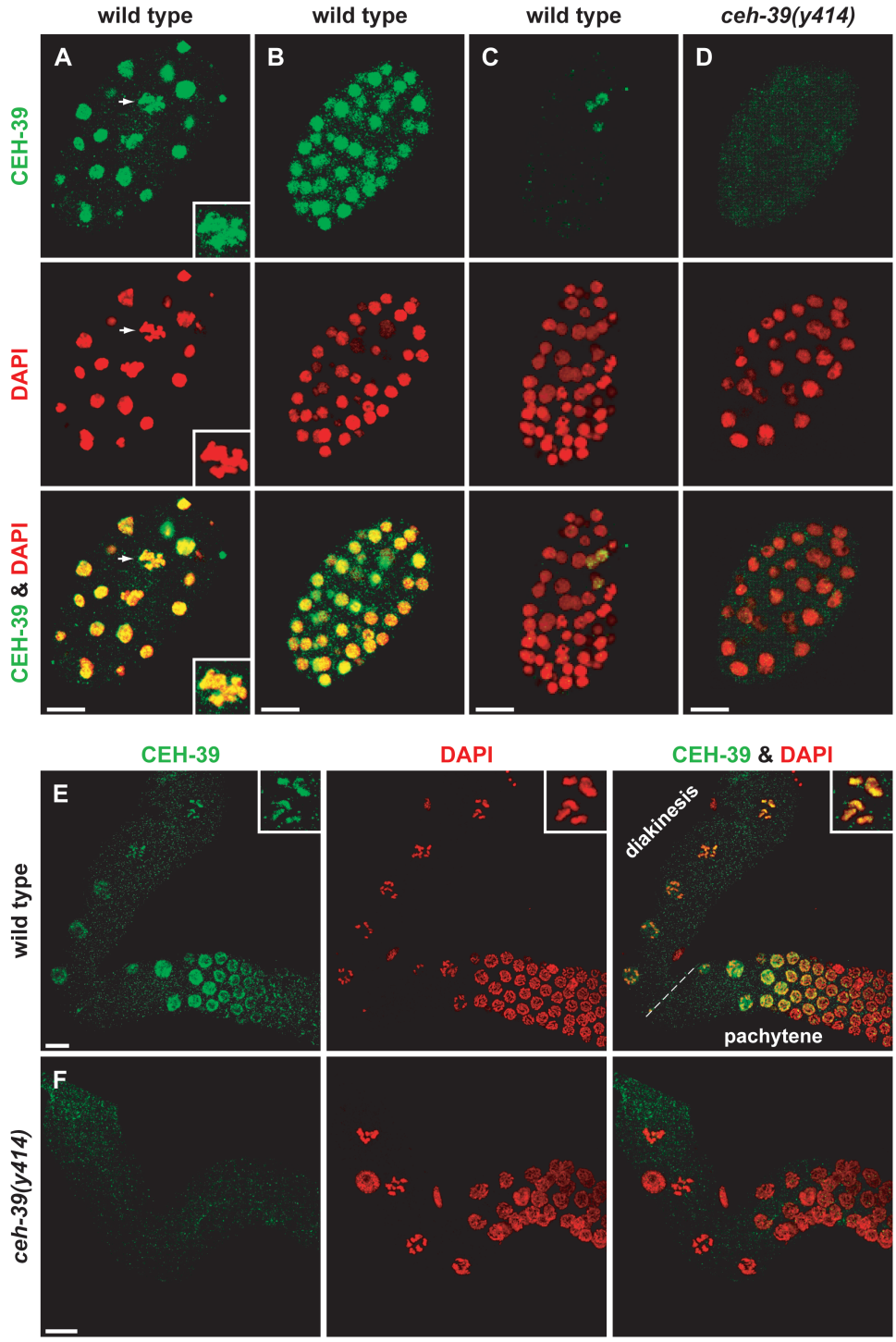

FIGURE 4.—CEH-39 accumulates in nuclei of young embryos, consistent with its role as an XSE, and also in germline nuclei. (A–D) Partial projections of false-colored confocal images of wild-type and *ceh-39* mutant embryos stained with DAPI (red) and antibodies (CA1184) against CEH-39 (green). (A and B) CEH-39 localizes in a diffuse pattern within interphase nuclei of young (50-cell) and older (150- to 200-cell) XX embryos; CEH-39 also associates with mitotic chromosomes (arrow and inset in A). (C) CEH-39 is greatly reduced in embryos with >200 cells. (D) No CEH-39 antibody staining was detectable in *ceh-39* deletion mutant embryos, which lack the antibody epitope, demonstrating specificity of the CEH-39 antibody. Bars, 10 μm. (E and F) Partial projections of false-colored confocal images of wild-type and *ceh-39* mutant gonads stained with DAPI (red) and CEH-39 antibodies (green) (CA1183). Two focal planes (separated by a dashed white line in E) were used to show pachytene and diplotene diakinesis. In late pachytene and early diplotene, CEH-39 staining appears diffuse nuclear and excluded from the nucleolus. In late diplotene and diakinesis, staining colocalizes with condensed chromosomes. Enlargement of the nucleus in diakinesis is shown in insets in E. Staining is absent in gonads of *ceh-39* deletion mutants.

effect on the derepression of *yIs33* by *sex-1* mutations, consistent with CEH-39 acting through *xol-1* sequences not in the promoter. That is, an equivalent number of hermaphrodites produced embryos expressing high levels of *lacZ* in both the *yIs33; sex-1(y263)* strain and the *yIs33; yIs58/yIs58; sex-1(y263)* strain (Figure 5D). These results show *ceh-39* to be a repressor of *xol-1* that acts independently of *sex-1*. The function of CEH-39, but not that of SEX-1, depends on sequences spanning the first three exons of *xol-1*.

***ceh-39* and other XSEs reduce *xol-1* transcript levels:** The changes observed in the expression of *xol-1* reporters show that *ceh-39* represses *xol-1* but do not establish whether *ceh-39* regulates *xol-1* transcript levels. Therefore, qRT–PCR was used to measure the total level of *xol-1* transcripts in both wild-type and XSE mutant XX embryos using *xol-1* primer sets designed to measure all splice variants of *xol-1* simultaneously (Table 7).

Mutations that inactivate transcriptional repressors of *xol-1* should increase *xol-1* transcripts, but mutations

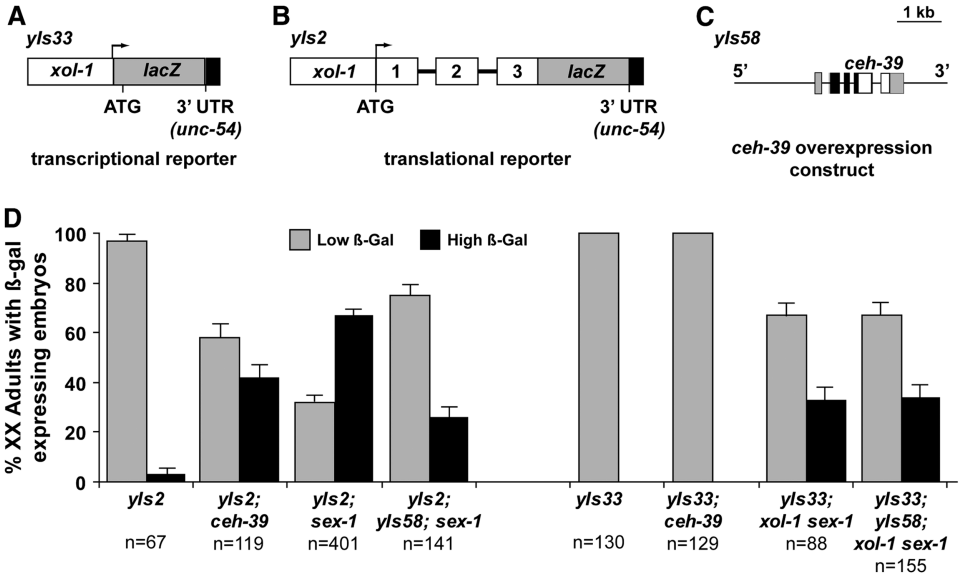

FIGURE 5.—*ceh-39* represses *xol-1* expression via genomic sequences spanning the first three exons of *xol-1*. (A) *yIs33* is an integrated *xol-1* transcriptional reporter transgene containing the *xol-1* promoter (2.8 kbp) (open box) fused in-frame to the *lacZ* gene (shaded box) and the *unc-54* 3′-UTR (solid box). (B) *yIs2* is an integrated *xol-1* translational reporter transgene containing the *xol-1* promoter (2.8 kbp) and genomic sequences spanning the first three exons of *xol-1* fused in-frame with the *lacZ* gene (shaded box) and the *unc-54* 3′-UTR (solid box). The promoter and exons are represented by open boxes and introns by lines. Both *y1s2* and *yIs33* recapitulate the regulation of *xol-1*: high expression in XO embryos and low expression in XX embryos. (C) *yIs58* is an integrated *ceh-39*-overexpressing transgene containing a 5.5-kbp genomic fragment spanning the *ceh-39* promoter (2.3 kbp), coding region, and 1 kbp of downstream sequence. (D) β-Galactosidase levels were qualitatively estimated and binned for *sex-1*, *ceh-39*, and *yIs58; sex-1* mutant animals carrying either *yIs2* or *yIs33*. A *xol-1* mutation was included in strains with *yIs33* and a *sex-1* mutation to suppress the synergistic XX lethality. XX embryos were considered to have high levels of β-galactosidase activity if the intensity of staining matched that of XO animals and low levels of β-galactosidase activity if the staining ranged from none to less intense than that of XO animals. Both *sex-1* and *ceh-39* mutants derepress *yIs2*, as assessed by the increased percentages of adults bearing embryos strongly expressing β-galactosidase; *sex-1* and *ceh-39* must repress *xol-1* through sequences present in *yIs2*. Overexpressing CEH-39 via *yIs58* reduced the percentage of *sex-1* mutant adults expressing β-galactosidase, indicating that increased levels of CEH-39 can restore repression to *xol-1* in the absence of *sex-1* through *xol-1* genomic sequences spanning the first three exons. In contrast, *ceh-39* mutants did not derepress the *xol-1* transcriptional reporter *yIs33*, unlike *sex-1* mutants. Consistent with this finding, overexpressing CEH-39 via *yIs58* did not restore *xol-1* repression in *sex-1* mutants, indicating that *ceh-39* does repress *xol-1* through its promoter sequences. Error bars represent the standard deviation of a binomial distribution.

that disrupt post-transcriptional regulators should not. Our data show that *ceh-39*, *sex-1*, and *sex-2* regulate total *xol-1* transcript levels, but *fox-1* does not (Table 7).

xol-1 expression is 10 times lower in XX than in XO embryos (RHIND *et al.* 1995). Since XSEs act cumulatively, mutations in individual XSEs would be expected to increase *xol-1* transcript levels <10-fold compared to wild-type levels. In fact, a *sex-1* mutation caused an increase in *xol-1* transcript levels 3-fold above wild-type levels ($P < 0.01$), consistent with a role as a transcriptional repressor, while a *fox-1* mutation had no obvious effect on *xol-1* transcript levels, as expected from its role as a post-transcriptional regulator (Table 7). Both deletion alleles of *ceh-39* increased *xol-1* transcript levels ~2-fold above wild-type levels in XX embryos ($P < 0.01$, Table 7). Together with *xol-1* reporter data, these results indicate that *ceh*-39 regulates *xol-1* transcript levels either directly through a regulatory element present in the genomic sequence spanning the first three exons of *xol-1* or indirectly by unknown means.

The XSE *sex-2* also affects the total level of *xol-1* transcripts. A *sex-2* mutation, like a *ceh-39* mutation, increased *xol-1* transcript levels approximately twofold above wild-type levels in XX embryos ($P < 0.01$; Table 7). These results show that four of five XSEs affect *xol-1* transcript levels. Repression of *xol-1* transcript levels appears to be the most prevalent mode of *xol-1* regulation by XSEs; however, post-transcriptional repression by XSEs such as *fox-1* plays an important role in *xol-1* regulation (Figure 6; Tables 3, 5, and 7; NICOLL *et al.* 1997; CARMI and MEYER 1999).

DISCUSSION

We addressed the fundamental question of how a small difference in the concentration of an intracellular signal is amplified to induce different cell fates. In *C. elegans*, sex is determined through a dose-dependent signal that translates the twofold difference in X chromosome dose between XO and XX diploid embryos into the male or hermaphrodite fate by switching the *xol-1* sex-determination gene on or off. The sex signal, the X:A ratio, consists of autosomal signal elements that activate *xol-1* and of X signal elements that repress it. In this study, we identified the X signal element CEH-39, a ONECUT homeodomain transcription factor. CEH-39 functions in the sex-determination pathway upstream of *xol-1* to communicate X chromosome dose by repressing *xol-1* transcript levels in a dose-dependent manner. Furthermore, we showed that four of the five known

TABLE 7

XSE mutations increase *xol-1* transcript levels

Genotype	Transcript measuredby qRT–PCR[a]	
	xol-1	*nhr-64*
sex-1(y263)	3.0 ± 0.5	1.1 ± 0.1
sex-2(y324)	1.8 ± 0.2	1.2 ± 0.1
ceh-39(y414)	2.0 ± 0.2	1.1 ± 0.1
ceh-39(gk296)	2.0 ± 0.3	1.1 ± 0.1
fox-1(y303)	1.0 ± 0.1	1.3 ± 0.1

[a] The levels of *xol-1* and XSE transcripts in mutant embryos (listed by genotype) were measured by qRT–PCR and are expressed as the fold change compared to the transcript levels measured in wild-type embryos (see MATERIALS AND METHODS). For example, a value of 2.0 means that twice as many gene-specific transcripts were measured in mutant embryos than in wild-type embryos. All transcript levels were normalized to the levels of the control gene, *fasn-1* (ORF F32H2.5), whose expression is constant throughout embryogenesis and is not affected by dosage compensation. See VAN GILST *et al.* (2005) for details and protocol. *nhr-64*, another gene not affected by dosage compensation, was used as a control to gauge the variability and reliability of measurements made using qRT–PCR. Experimental error is expressed as the standard error of the mean. A critical control was to compare the *fasn-1*-normalized *xol-1* or *nhr-64* transcript levels in three independent preparations of wild-type embryos. That comparison showed the *xol-1* and *nhr-64* transcript levels to be statistically equivalent among the independent RNA preparations (*xol-1*, 1.2 ± 0.2; *nhr-64*, 1.3 ± 0.1).

XSEs control *xol-1* at this level of regulation, suggesting that the sensitivity of the sex-determination signal stems in part from synergistic interactions among multiple repressors acting at the transcript level.

Function of the ONECUT homeodomain protein CEH-39 in determining sex: OC homeodomain proteins are a conserved class of transcription factors that normally contain a bipartite DNA-binding domain composed of a single cut domain and an atypical homeodomain (LEMAIGRE *et al.* 1996; BURGLIN and CASSATA 2002). OC proteins can stimulate transcription by recruiting the CREB-binding protein coactivator through an LXXLL motif in the cut domain (LANNOY *et al.* 2000). The OC DBD can also function as a coactivator with the Forkhead box family of transcription factors, which contain winged-helix DBDs (RAUSA *et al.* 2003). Although most OC proteins act as transcriptional activators, at least one example exists in which an OC protein acts to inhibit transcription rather than stimulate it, by antagonizing the activity of another transcription factor (PIERREUX *et al.* 1999).

Here we have demonstrated the function of an OC protein as a dose-dependent repressor. The DBD of CEH-39 is similar to other OC proteins in organisms as diverse as insects and mammals, yet outside the DBD, CEH-39 bears no similarity to other OC proteins, including CEH-21 and CEH-41, two *C. elegans* OC proteins encoded in an operon with CEH-39 (BURGLIN and CASSATA 2002). Both CEH-21 and CEH-41 contain the conserved sequence element OCAM (ONECUT-associated motif) that CEH-39 lacks, and *ceh-41* lacks the cut domain in its DBD. Functional analysis showed that, of the three coregulated OC genes, only *ceh-39* functions as an XSE. Disruption of neither *ceh-21* nor *ceh-41* had any affect on sex determination or dosage compensation in the sensitized XX and XO genetic backgrounds used.

CEH-39's action as a dose-dependent repressor of *xol-1* transcript levels requires a 350-bp region of *xol-1* spanning its first three exons, thus identifying new sites of *xol-1* important for the control of its transcript levels. Previous analysis of SEX-1 revealed that transcriptional regulation of *xol-1* occurred through its promoter (CARMI *et al.* 1998). Similarly, other *xol-1* regions might also be necessary for regulation by CEH-39, but they are not sufficient to confer repression without this 350-bp region. Thus, in its capacity as a transcriptional repressor, CEH-39 could, in principle, bind not only to *cis* regulatory elements outside the *xol-1* promoter, but also to ones within the promoter. The 350-bp region contains two core consensus binding sites (ATCAAT) established for the mammalian OC protein HNF-6 (LANNOY *et al.* 1998). The *C. elegans* OC protein CEH-21 binds to DNA sequences containing this consensus site (LANNOY *et al.* 1998), indicating that OC-binding specificity is evolutionarily conserved. Since both *ceh-39* and *ceh-21* encode bipartite OC DBDs, it is likely that CEH-39 also binds sequences bearing ATCAAT. These consensus binding sites reside in the *xol-1* promoter as well as within the first three exons, providing the opportunity for cooperation in the binding of CEH-39 molecules to distant sites within the *xol-1* locus. Indeed, preliminary electromobility shift assays using the recombinant CEH-39 protein suggest that CEH-39 binds to multiple, OC consensus-like sites in the *xol-1* promoter and in exon 3.

Function of the X signal: Our work has shown that transcriptional regulation is the predominant but not exclusive form of *xol-1* repression by the multi-genic X signal (Figure 6). Previous analysis had predicted that the XSE in region 2 would regulate *xol-1* at the post-transcriptional level and that transcriptional and post-transcriptional regulation might be equally important (NICOLL *et al.* 1997). The discovery of the CEH-39 transcriptional regulator in region 2 and the observation that *sex-2* also controls *xol-1* transcript levels suggests that more XSEs control *xol-1* at the transcriptional level rather than at the post-transcriptional level. However, at least one XSE, the RNA-binding protein FOX-1, is a potent post-transcriptional regulator of *xol-1*, indicating that multiple levels of regulation function to relay the X signal to the sex determination and dosage compensation machinery. The combined action of two separate mechanisms enhances *xol-1* repression.

Studies of multi-component nucleoprotein complexes, called enhanceosomes and repressosomes, which activate or repress transcription in eukaryotes, may provide

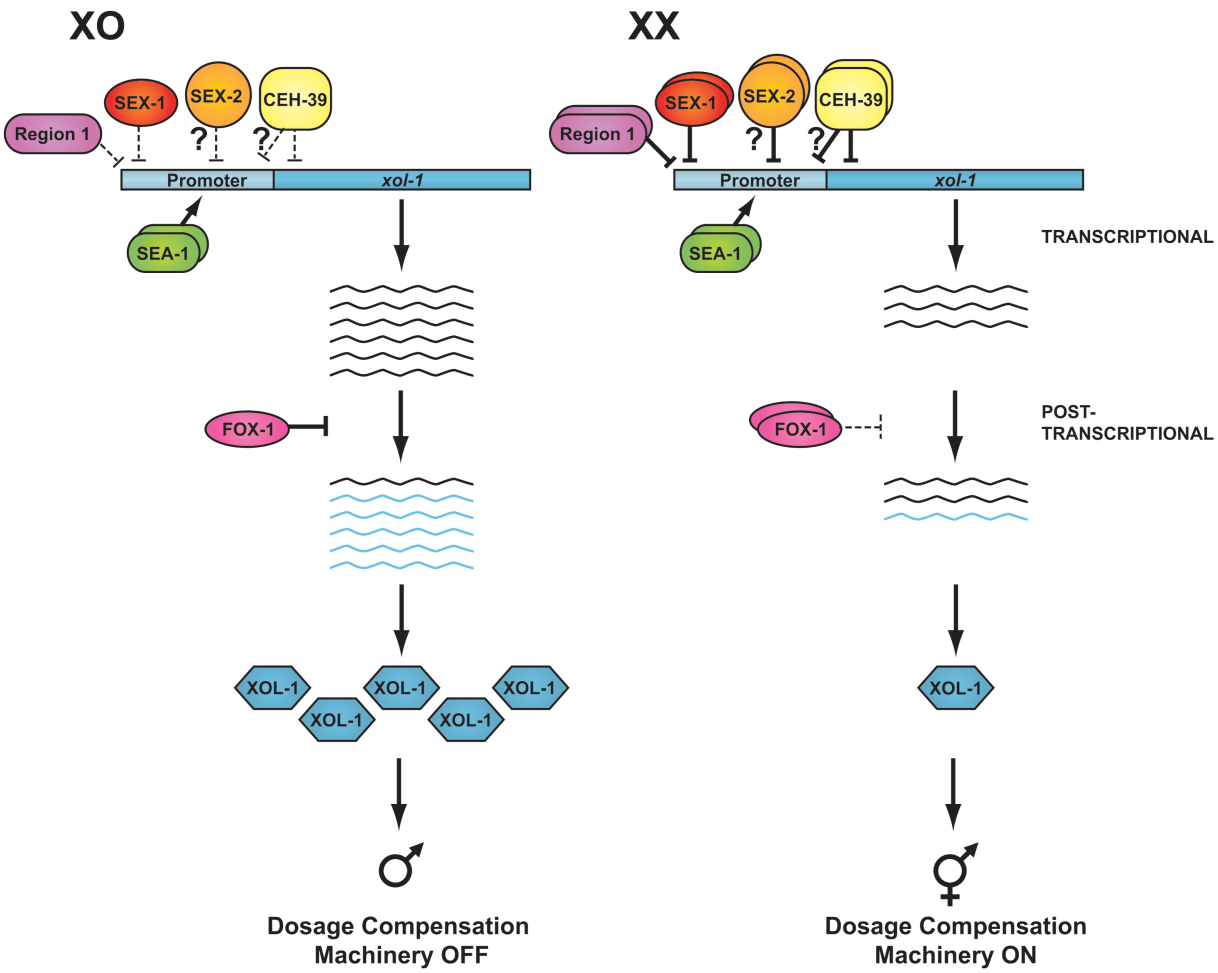

FIGURE 6.—Regulation of *xol-1* through XSEs and ASEs. *xol-1* is the direct molecular target of the X:A signal and integrates both X and autosomal components to determine sexual fate. The molecular diagram indicates where the XSEs act to repress *xol-1* and where the ASEs function to activate *xol-1*. Our study showed that CEH-39 and most other XSEs communicate X chromosome dose by repressing *xol-1* transcript levels. The XSE in region 1 and SEX-1 (nuclear hormone receptor) repress *xol-1* through sequences in the promoter, while CEH-39 (homeodomain protein) acts through *xol-1* genomic sequences that span the first three exons. CEH-39 may also function through promoter sequences. The means by which *sex-2* represses *xol-1* transcript levels has not been defined. Using a separate mechanism, FOX-1, an RNA-binding protein, represses *xol-1* on a post-transcriptional level. Both the transcriptional and post-transcriptional mechanism are important for *xol-1* repression. The ASE SEA-1 (T-box protein) activates *xol-1* transcript levels using promoter sequences. XSEs and ASEs could compete directly to regulate *xol-1* by binding overlapping or neighboring *cis* regulatory sites or indirectly by affecting components of the transcriptional machinery. The end result is that the higher XSE activity in XX animals out-competes ASE activity and inactivates *xol-1*, but the lower XSE activity in XO animals permits the ASE activity to activate *xol-1*. The high level of XOL-1 protein present in XO animals then induces the male fate, including repression of the dosage compensation machinery. The lower level of XOL-1 in XX animals permits the hermaphrodite fate, including activation of the dosage compensation machinery.

a molecular explanation for the phenotypic synergy observed among XSEs. Cooperative binding of multiple independent activators or repressors to each other and to DNA leads to synergistic changes in transcription by, for example, altering the recruitment of the basal RNA polymerase II transcriptional machinery to a promoter (CAREY 1998; PTASHNE and GANN 2002; GOWRI *et al.* 2003; PTASHNE 2004). The result of this synergy is that small changes in the concentration of multiple regulators causes a greater-than-additive transcriptional response of their target gene. The fact that XSEs function synergistically and that at least four XSEs (*ceh-39*, *sex-1*, *sex-2*, and the XSE in region 1) affect *xol-1* transcript levels opens the possibility that these XSEs function as part of a repressosome recruited to *xol-1* regulatory regions.

Our genetic evidence indicates that *ceh-39* functions both independently of *sex-1* and synergistically with it to repress *xol-1*. These two XSEs require different sites in the *xol-1* locus to regulate it. SEX-1, a nuclear hormone receptor, represses *xol-1* transcription through its binding sites in the *xol-1* promoter (CARMI *et al.* 1998). CEH-39 requires *xol-1* sequences spanning the first three exons to repress it, although OC consensus binding

motifs occur in both the promoter and the exons, suggesting that CEH-39 could actually bind to either or both locations. Thus, the possibility exists for CEH-39 and SEX-1 to bind *xol-1* in a cooperative manner. However, the fact that *ceh-39* and *sex-1* may potentially bind nonadjacent sites in the *xol-1* locus suggests that if they are part of a repressosome, (1) their binding may change DNA structure to bring the sites into close proximity or (2) the two XSEs may collaborate indirectly through interactions with the general transcriptional machinery.

XSEs *vs.* ASEs: The question arises as to why so many XSEs regulate *xol-1* transcript levels. The recent characterization of ASEs provides a clue. Loss of the two known ASEs (*sea-1* and *sea-2*) reduces *xol-1* transcript levels, suggesting that a significant component of the autosomal signal activates *xol-1* through transcriptional mechanisms (Powell *et al.* 2005; P. Nix and B. J. Meyer, unpublished results). With both the X and autosomal components of the primary sex signal regulating *xol-1* at the level of transcription, these opposing elements could compete for the control of the regulatory machinery that sets *xol-1* expression levels. XSEs and ASEs could compete directly by binding overlapping or neighboring *cis* regulatory targets or indirectly by influencing components of the transcriptional machinery. Direct competition could endow XSEs and ASEs with the dose sensitivity necessary to assess X chromosome number. The signal with the higher activity could out-compete the opposing signal and gain control of *xol-1* expression. In XX animals, the high XSE activity would inactivate *xol-1*, but in XO animals, the lower XSE activity would permit the relatively higher ASE activity to turn on *xol-1*.

Relative strength of XSEs: XSEs function cumulatively to repress *xol-1*, and an individual XSE appears to contribute a relatively small portion of the X signal, thus accounting, in part, for the large number of XSEs (at least five). However, not all XSEs contribute equally to the X signal; their relative strengths differ significantly. *sex-1* appears to make the strongest individual contribution: loss of *sex-1* activity causes substantial XX-specific lethality, unlike the loss of any other single XSE. In fact, *sex-1* appears stronger than *ceh-39*, *fox-1*, and *sex-2* combined. Paradoxically, a *sex-1* mutation derepresses *xol-1* transcript levels by only 1.5-fold more than an XSE mutation that causes insignificant XX lethality. Furthermore, even though *ceh-39* overexpression rescues the lethality of *sex-1* mutants and reduces *xol-1* transcript levels to that of *ceh-39* mutants (Figure 5), which have no overt phenotype, the *ceh-39*-overexpressing *sex-1* mutants are still somewhat Dpy. How can that be? The fact that these mutants are still Dpy despite low *xol-1* transcript levels suggests that *sex-1*'s role in the sex-determination pathway may be multi-faceted. *sex-1* may affect the sex-determination pathway independently of *xol-1*. If *sex-1* has a dual role as an XSE and a *xol-1* independent regulator of sex determination and dosage compensation, then mutations in *sex-1* (1) would cause phenotypes more severe than expected on the basis of its effects on *xol-1* expression and (2) would not be completely suppressed by increasing the dose of another XSE. Both appear to be true, and further analysis of *sex-1* in the accompanying article in this issue (Gladden *et al.* 2007) establishes the involvement of *sex-1* in other aspects of sex determination and dosage compensation.

In summary, our analysis of the dose-dependent sex-determination signal in *C. elegans* revealed important insights into the strategy by which the twofold difference in X dose between XO and XX animals is translated into the male *vs.* hermaphrodite fate by rendering *xol-1* active or inactive. We identified a new component of the X signal, *ceh-39*, and showed that the dose dependence of the sex-determination signal derives in part from the regulation of *xol-1* transcript levels by multiple, independent XSEs.

We thank M. Van Gilst for guidance with quantitative RT–PCR, D. King for designing and producing the CEH-39 peptide for antibody production, P. Nix for providing strains and information about ASEs, J. Powell and C. Y. Loh for strains and information about *sex-2*, the *C. elegans* Gene Knockout Consortium for providing the *ceh-39(gk296)* mutant, T. Cline for discussions, and I. Carmi, B. Farboud, M. Jow, and A. Severson for critical comments on the manuscript. This work was supported by National Institutes of Heath grant GM30702 to B.J.M. and by a National Science Foundation Predoctoral Fellowship to J.M.G. B.J.M. is an investigator of the Howard Hughes Medical Institute.

LITERATURE CITED

Akerib, C. C., and B. J. Meyer, 1994 Identification of X chromosome regions in *Caenorhabditis elegans* that contain sex-determination signal elements. Genetics **138:** 1105–1125.

Blumenthal, T., D. Evans, C. D. Link, A. Giffanti, D. Lawson *et al.*, 2002 A global analysis of *Caenorhabditis elegans* operons. Nature **417:** 851–854.

Brenner, S., 1974 The genetics of *Caenorhabditis elegans*. Genetics **77:** 71–94.

Burglin, T. R., and G. Cassata, 2002 Loss and gain of domains during evolution of cut superclass homeobox genes. Int. J. Dev. Biol. **46:** 115–123.

Carey, M., 1998 The enhanceosome and transcriptional synergy. Cell **92:** 5–8.

Carmi, I., and B. J. Meyer, 1999 The primary sex determination signal of *Caenorhabditis elegans*. Genetics **152:** 999–1015.

Carmi, I., J. B. Kopczynski and B. J. Meyer, 1998 The nuclear hormone receptor SEX-1 is an X-chromosome signal that determines nematode sex. Nature **396:** 168–173.

Chu, D. S., H. E. Dawes, J. D. Lieb, R. C. Chan, A. F. Kuo *et al.*, 2002 A molecular link between gene-specific and chromosome-wide transcriptional repression. Genes Dev. **16:** 796–805.

Chuang, P. T., D. G. Albertson and B. J. Meyer, 1994 DPY-27: a chromosome condensation protein homolog that regulates *C. elegans* dosage compensation through association with the X chromosome. Cell **79:** 459–474.

Cline, T. W., and B. J. Meyer, 1996 Vive la différence: males vs. females in flies vs. worms. Annu. Rev. Genet. **30:** 637–701.

Csankovszki, G., P. McDonel and B. J. Meyer, 2004 Recruitment and spreading of the *C. elegans* dosage compensation complex along X chromosomes. Science **303:** 1182–1185.

Davis, T. L., and B. J. Meyer, 1997 SDC-3 coordinates the assembly of a dosage compensation complex on the nematode X chromosome. Development **124:** 1019–1031.

Dawes, H. E., D. S. Berlin, D. M. Lapidus, C. Nusbaum, T. L. Davis *et al.*, 1999 Dosage compensation proteins targeted to X

chromosomes by a determinant of hermaphrodite fate. Science **284:** 1800–1804.

Delong, L., J. D. Plenefisch, R. D. Klein and B. J. Meyer, 1993 Feedback control of sex determination by dosage compensation revealed through *Caenorhabditis elegans sdc-3* mutations. Genetics **133:** 875–896.

Gladden, J. M., B. Farboud and B. J. Meyer, 2007 Revisiting the X:A signal that specifies *Caenorhabditis elegans* sexual fate. Genetics **177:** 1639–1654.

Gowri, P. M., J. H. Yu, A. Shaufl, M. A. Sperling and R. K. Menon, 2003 Recruitment of a repressosome complex at the growth hormone receptor promoter and its potential role in diabetic nephropathy. Mol. Cell. Biol. **23:** 815–825.

Hirano, T., 1999 SMC-mediated chromosome mechanics: A conserved scheme from bacteria to vertebrates? Genes. Dev. **13:** 11–19.

Hodgkin, J., H. R. Horvitz and S. Brenner, 1979 Nondisjunction mutants of the nematode *Caenorhabditis elegans*. Genetics **91:** 67–94.

Hodgkin, J., J. D. Zellan and D. G. Albertson, 1994 Identification of a candidate primary sex determination locus, *fox-1*, on the X chromosome of *Caenorhabditis elegans*. Development **120:** 3681–3689.

Howe, M., K. L. McDonald, D. G. Albertson and B. J. Meyer, 2001 HIM-10 is required for kinetochore structure and function on *Caenorhabditis elegans* holocentric chromosomes. J. Cell Biol. **153:** 1227–1238.

Hsu, D. R., and B. J. Meyer, 1994 The *dpy-30* gene encodes an essential component of the *Caenorhabditis elegans* dosage compensation machinery. Genetics **137:** 999–1018.

Kamath, R. S., and J. H. Ahringer, 2003 Genome-wide RNAi screening in *Caenorhabditis elegans*. Methods **4:** 313–321.

Kamath, R. S., M. Martinez-Campos, P. Zipperlen, A. G. Fraser and J. Ahringer, 2001 Effectiveness of specific RNA-mediated interference through ingested double-stranded RNA in *Caenorhabditis elegans*. Genome Biol. **2:** RESEARCH0002.

Kimura, K., and T. Hirano, 1997 ATP-dependent positive supercoiling of DNA by 13S condensin: a biochemical implication for chromosome condensation. Cell **90:** 625–634.

Lannoy, V. J., T. R. Burglin, G. G. Rousseau and F. P. Lemaigre, 1998 Isoforms of hepatocyte nuclear factor-6 differ in DNA-binding properties, contain a bifunctional homeodomain, and define the new ONECUT class of homeodomain proteins. J. Biol. Chem. **273:** 13552–13562.

Lannoy, V. J., A. Rodolosse, C. E. Pierreux, G. G. Rousseau and F. P. Lemaigre, 2000 Transcriptional stimulation by hepatocyte nuclear factor-6 target-specific recruitment of either CREB-binding protein (CBP) or p300/CBP-associated factor (p/CAF). J. Biol. Chem. **275:** 22098–22103.

Lemaigre, F. P., S. M. Durviaux, O. Truong, V. J. Lannoy, J. J. Hsuan *et al.*, 1996 Hepatocyte nuclear factor 6, a transcription factor that contains a novel type of homeodomain and a single cut domain. Proc. Natl. Acad. Sci. USA **93:** 9460–9464.

Lieb, J. D., E. E. Capowski, P. Meneeley and B. J. Meyer, 1996 DPY-26, a link between dosage compensation and meiotic chromosome segregation in the nematode. Science **274:** 1732–1736.

Lieb, J. D., M. R. Albrecht, P. T. Chuang and B. J. Meyer, 1998 MIX-1: an essential component of the *C. elegans* mitotic machinery executes X chromosome dosage compensation. Cell **92:** 265–277.

Lynch, J., and C. Desplan, 2003 'De-evolution' of Drosophila toward a more generic mode of axis patterning. Int. J. Dev. Biol. **47:** 497–503.

Madl, J. E., and R. K. Herman, 1979 Polyploids and sex determination in *Caenorhabditis elegans*. Genetics **93:** 393–402.

McDonel, P. E., J. Jans, B. K. Peterson and B. J. Meyer, 2006 Clustered DNA motifs mark X chromosomes for repression by a dosage compensation complex. Nature **444:** 614–618.

McKim, K. S., A. M. Howell and A. M. Rose, 1988 The effects of translocations on recombination frequency in *Caenorhabditis elegans*. Genetics **120:** 987–1001.

Meyer, B. J., 2005 X-chromosome dosage compensation, in *WormBook*, edited by The *C. elegans* Research Community. http://www.wormbook.org.

Miller, L. M., J. D. Plenefisch, L. P. Casson and B. J. Meyer, 1988 *xol-1*: a gene that controls the male modes of both sex determination and X chromosome dosage compensation in *C. elegans*. Cell **55:** 167–183.

Nicoll, M., C. C. Akerib and B. J. Meyer, 1997 X-chromosome-counting mechanisms that determine nematode sex. Nature **388:** 200–204.

Nonet, M., and B. J. Meyer, 1991 Early aspects of *Caenorhabditis elegans* sex determination and dosage compensation are regulated by a zinc-finger protein. Nature **351:** 65–68.

Nusbaum, C., and B. J. Meyer, 1989 The *Caenorhabditis elegans* gene *sdc-2* controls sex determination and dosage compensation in XX animals. Genetics **122:** 579–593.

Parisi, M., and H. Lin, 2000 Translational repression: a duet of Nanos and Pumilio. Curr. Biol. **10:** R81–R83.

Pierreux, C. E., J. Stafford, D. Demonte, D. K. Scott, J. Vandenhaute *et al.*, 1999 Antiglucocorticoid activity of hepatocyte nuclear factor-6. Proc. Natl. Acad. Sci. USA **96:** 8961–8966.

Plenefisch, J. D., L. Delong and B. J. Meyer, 1989 Genes that implement the hermaphrodite mode of dosage compensation in *Caenorhabditis elegans*. Genetics **121:** 57–76.

Powell, J., M. Jow and B. Meyer, 2005 The T-box transcription factor SEA-1 is an autosomal element of the X:A signal that determines *C. elegans* sex. Dev. Cell **9:** 339–349.

Ptashne, M., 2004 *A Genetic Switch*. Cold Spring Harbor Laboratory Press, Cold Spring Harbor, NY.

Ptashne, M., and A. Gann, 2002 *Genes & Signals*. Cold Spring Harbor Laboratory Press, Cold Spring Harbor, NY.

Rausa, F. M., Y. Tan and R. H. Costa, 2003 Association between hepatocyte nuclear factor 6 (HNF-6) and FoxA2 DNA binding domains stimulates FoxA2 transcriptional activity but inhibits HNF-6 DNA binding. Mol. Cell. Biol. **23:** 437–449.

Rhind, N. R., L. M. Miller, J. B. Kopczynski and B. J. Meyer, 1995 *xol-1* acts as an early switch in the *C. elegans* male/hermaphrodite decision. Cell **80:** 71–82.

Riddle, D. L., T. Blumenthal, B. J. Meyer and J. R. Priess, 1997 *C. elegans II*. Cold Spring Harbor Laboratory Press, Cold Spring Harbor, NY.

Van Gilst, M. R., H. Hadjivassiliou, A. Jolly and K. R. Yamamoto, 2005 Nuclear hormone receptor NHR-49 controls fat consumption and fatty acid composition in *C. elegans*. PLoS Biol. **3:** e53.

Villeneuve, A. M., and B. J. Meyer, 1987 *sdc-1*: a link between sex determination and dosage compensation in *C. elegans*. Cell **48:** 25–37.

Villeneuve, A. M., and B. J. Meyer, 1990 The role of *sdc-1* in the sex determination and dosage compensation decisions in *Caenorhabditis elegans*. Genetics **124:** 91–114.

Yonker, S. A., and B. J. Meyer, 2003 Recruitment of *C. elegans* dosage compensation proteins for gene-specific versus chromosome-wide repression. Development **130:** 6519–6532.

Communicating editor: D. I. Greenstein